
Theses and Dissertations

Fall 2014

Uptake, translocation, and toxicity of gold nanorods in maize

Nastaran Moradi Shahmansouri
University of Iowa

Follow this and additional works at: <https://ir.uiowa.edu/etd>



Part of the [Civil and Environmental Engineering Commons](#)

Copyright © 2014 Nastaran Moradi Shahmansouri

This thesis is available at Iowa Research Online: <https://ir.uiowa.edu/etd/1488>

Recommended Citation

Moradi Shahmansouri, Nastaran. "Uptake, translocation, and toxicity of gold nanorods in maize." MS (Master of Science) thesis, University of Iowa, 2014.
<https://doi.org/10.17077/etd.hkyxv8ko>

Follow this and additional works at: <https://ir.uiowa.edu/etd>



Part of the [Civil and Environmental Engineering Commons](#)

**UPTAKE, TRANSLOCATION, AND TOXICITY OF GOLD NANORODS
IN MAIZE**

by

Nastaran Moradi Shahmansouri

A thesis submitted in partial fulfillment
of the requirements for the Master of
Science degree in Civil and Environmental Engineering in the Graduate College
The University of Iowa

December 2014

Thesis Supervisor: Professor Jerald L. Schnoor

Copyright by

NASTARAN MORADI SHAHMANSOURI

2014

All Rights Reserved

Graduate College
The University of Iowa
Iowa City, Iowa

CERTIFICATE OF APPROVAL

MASTER'S THESIS

This is to certify that the Master's thesis of

Nastaran Moradi Shahmansouri

has been approved by the Examining Committee
for the thesis requirement for the Master of Science
degree in Civil and Environmental Engineering at
the December 2014 graduation.

Thesis Committee:

Jerald L. Schnoor, Thesis Supervisor

A. Allen Bradley, Jr.

Guangshu Zhai

To my family and friends for all their endless support and to my best friend CJ Huang for all of his patience, love, and encouragement.

ACKNOWLEDGEMENTS

I would like to express my deepest appreciation to my advisor, Jerry Schnoor for his guidance, patience, and knowledge.

I would like to thank Dr. David Peate for all his help on ICP-MS analysis. I would also like to thank Katherine Walter for guiding me through the TEM microscopy processes.

I am most grateful to Dr. Guangshu Zhai and Meaghan Kern for their help during my research, to John Durst and Erric Jetter for their support in the lab, and to all of civil and environmental department for creating the atmosphere to learn and research.

ABSTRACT

Nanomaterials are widely used in many different products, such as electronics, cosmetics, industrial goods, biomedical uses, and other material applications. The heavy emission of nanomaterials into the environment has motivated increasing concern regarding the effects on ecosystems, food chains, and, human health. Plants can tolerate a certain amount of natural nanomaterials, but large amounts of ENMs released from a variety of industries could be toxic to plants and possibly threaten the ecosystem.

Employing phytoremediation as a contamination treatment method may show promise. However a pre-requisite to successful treatment is a better understanding of the behavior and effects of nanomaterials within plant systems. This study is designed to investigate the uptake, translocation, bioavailability, and toxicity of gold nanorods in maize plants. Maize is an important food and feed crop that can be used to understand the potential hazardous effects of nanoparticle uptake and distribution in the food chain. The findings could be an important contribution to the fields of phytoremediation, agri-nanotechnology, and nanoparticle toxicity on plants.

In the first experiment, hydroponically grown maize seedlings were exposed to similar doses of commercial non-coated gold nanorods in three sizes, 10x34 nm, 20x75 nm, and 40x96 nm. The three nanorod species were suspended in solutions at concentrations of 350 mg/l, 5.8 mg/l, and 14 mg/l, respectively. Maize plants were exposed to all three solutions resulting in considerably lower transpiration and wet biomass than control plants. Likewise, dry biomass was reduced, but the effect is less pronounced than that of transpiration and wet biomass. The reduced transpiration and water content, which eventually proved fatal to exposed plants, were most

likely a result of toxic effect of gold nanorod, which appeared to physically hinder the root system. TEM images proved that maize plants can uptake gold particles and accumulate them in root and leaf cells. However, the translocation factor of gold nanorods from root to leaf was very low in this experiment.

In the second experiment, maize seedlings were exposed to different (lower) concentrations of gold nanorods measured at 4.5×10^{-3} mg/l, 0.45 mg/l, and 2.25 mg/l for 10 days. Transpiration and biomass measurements demonstrated that the higher concentration of gold nanorods caused lower water uptake and growth, but lower concentrations did not show a significant toxic effect. According to ICP-MS results, root systems of the exposed plants were surrounded by high concentrations of sorbed nanorods, which physically interfered with uptake pathways and, thus, inhibited plant growth and nutritional uptake.

PUBLIC ABSTRACT

Contaminated soil and water is one of the major environmental issues in the last decades. Due to increasing applications in industry and medicine, nano-materials are recent but serious components of man-made pollution. The effects of nano-material contamination on plant-life and the ecosystem is drawing the interest of many researchers, but better understanding of the toxicity, fate, and, transport of nano-materials in plants is still needed.

This study is designed to investigate the uptake, translocation, toxicity and bioavailability of gold nanorods in maize plants.

In the first experiment, maize seedlings were exposed to high concentrations of gold nanorods of a variety of sizes in hydroponic systems. In the second experiment, maize plants were exposed to different, lower concentrations of gold nanorods. Results demonstrated that high concentrations of gold nanorods can be toxic to maize plants and cause lower water uptake and growth which is most likely a toxic inhibitory effect of gold nanorods on maize plants roots. Also the TEM images of tissue samples from plants exposed to gold nanorods demonstrated that maize plants are able to uptake nanorods from the hydroponic system and accumulate them in root and leaf cells. Since maize is a common agriculture crop, which is widely consumed, toxic effects of NPs in the food chain are essential to be known and understood. Furthermore, findings from this research can be helpful for fields of study in phytoremediation and agri-nanotechnology.

TABLE OF CONTENTS

LIST OF TABLES.....	ix
LIST OF FIGURES.....	x
CHAPTER I OVERVIEW	1
1.2 Introduction:.....	1
CHAPTER II LITERATURE REVIEW	5
CHAPTER III GOALS AND OBJECTIVES.....	9
3.1 Objective 1:.....	9
3.2 Objective 2:.....	9
3.3 Objective 3:.....	9
3.4 Objective 4:.....	9
3.5 Objective 5:.....	10
CHAPTER IV METHODOLOGY	11
4.1 Chemicals and Supplies:.....	11
4.1.1 Seed:.....	11
4.1.2 Growth solution:.....	11
4.1.3 Gold nanorod:.....	12
4.2 Cultivation and Growth:	14
4.2.1 Seed Preparation:.....	14
4.2.2 Plant preparation:	16
4.3 Sampling:.....	16
4.3.1 Sampling for TEM:	16
4.3.2 TEM Preparation method:.....	17
4.3.3 Sampling for ICP-MS:	18
4.3.4 ICP-MS preparation method:	18
CHAPTER V EXPERIMENTAL PROCEDURE.....	21
5.1 Experiment 1:.....	21
5.2 Experiment 2:.....	22
CHAPTER VI RESULTS AND DISCUSSION	23
6.1 Experiment 1:.....	23
6.1.1 Appearance:.....	23
6.1.2 Transpiration:	25
6.1.3 Growth:	26
6.1.4 TEM Results:	28
6.2 Experiment 2:.....	39
6.2.1 Appearance:.....	39
6.2.2 Transpiration:	42
6.2.3 Growth of the plants:.....	43
6.2.4 TEM Result:.....	45
6.2.5 ICP-MS Result:	49
CHAPTER VII FUTURE WORKS.....	55
REFERENCES	56
APPENDIX:	61

LIST OF TABLES

table 1: Corn seed information	11
table 2: 0.1 strength hoagland solution contents for 12 l batch	12
table 3: Characteristics of gold nanorods used in experiment 1	13
table 4: Characteristics of gold nanorods used in experiment 2	13
table 5: TEM preparation procedure ((russell) modified by katherine walter).....	17

LIST OF FIGURES

.Figure 1: global flow of enms in 2010 (metric tons/ year) from manufacturing to applications and eventual disposal or release into the environment considering the high range of production estimates and releases. Life cycle stages from left (production of enms) to right (final disposal or release).	2
Figure 2: tem images taken of gold nanorods used in experiment 1. Left) 10x 34 nm. Middle) 20x 75 nm. Right) 40x 96 nm.	13
Figure 3: TEM images taken of gold nanorods used in experiment 2. (25 x 69 nm)	14
Figure 4: germinated seeds ready to be planted	15
Figure 5: germinated seeds planted in 20 ml glass vial.	15
Figure 6: joel jem- 1230 electron microscope used for tem imaging	18
Figure 7: thermo scientific icp-ms instrument used for analyzing data on this experiment	20
Figure 8: maize plants exposed to a) 350 mg/l. B) 5.8 mg/l. C) 14 mg/l gold nanorods. D) control. On day 2	24
Figure 9: maize plants exposed to a) 350 mg/l. B) 5.8 mg/l. C) 14 mg/l gold nanorods. D) control. On day 6	24
figure10: maize plants exposed to a) 350 mg/l. B) 5.8 mg/l. C) 14 mg/l gold nanorods. D) control. On day 10	25
Figure 11: cumulative transpiration of maize plants exposed to different size gold nanorods and controls in 10 days experiment (n=3)	26
Figure 12: wet biomass of maize plants exposed to different size gold nanorods on each time point. (n=3)	27
Figure 13: dry biomass of maize plants exposed to different size gold nanorods on each time point. (n=3)	28
Figure 14: tem images taken of hoagland solution exposed to medium size (20 x 75) gold nanorods (5.8 mg/l) on day 10	29
Figure 15: top) a gold nanorod in a leaf tissue sample from a maize plants exposed to 5.8 mg/l/ the size appears to be consistent with the nanorods used in the experiment, 20 x 75 nm. Bottom) control plants tissue sample with no nanorod detected	31
Figure 16: a gold nanorod in a root tissue sample from a maize plant exposed to 5.8 mg/l gold nanorods, 20 x 75 nm	32
Figure 17: a gold nanorod was detected in this root tissue sample from a maize plant exposed to 5.8 mg/l gold nanorods, 20 x 75 nm. (outside of the cell)	33
Figure 18: a gold nanorod was detected in this root tissue sample from a maize plants exposed to 5.8 mg/l of gold nanorods, 20 x 75 nm	34
Figure 19: a gold nanorod was detected on this root tissue sample from a maize plants exposed to 5.8 mg/l of gold nanorods, 20 x 75 nm	35
Figure 20: top and bottom left) a gold nanorod was detected on this root tissue sample from a maize plants exposed to 5. Mg/l of gold nanorods, 20 x 75 nm. Bottom right) tissue sample from control plants without any visible nanorods	36
Figure 21: maize plants exposed to gold nanorods on day 5. Blue label) plants exposed to 2.25 mg/l. Yellow label) control plants	40

Figure 22: maize plants exposed to gold nanorods on day 5. Left) 0.45 mg/l. Middle) 4.5×10^{-3} mg/l. Right) control plants	40
Figure 23: maize plants exposed to nanorods on day 10. Blue label) 2.25 mg/l. Yellow label) controls	41
Figure 24: maize plants exposed to nanorods on day 10. Left) 0.45 mg/l. Middle) 4.5×10^{-3} mg/l. Right) controls	41
Figure 25: cumulative transpiration of maize plants exposed to different concentrations of gold nanorod for 10 days (n=3)	42
Figure 26: average plants length on day 10 (n=3)	43
Figure 27: average plants wet biomass on day 5 and 10. All plants were growing during this time interval. (n=3)	44
Figure 28: average plants dry biomass on days 5 and 10. All plants were growing during this time interval. (n=3)	44
Figure 29: TEM image of solution sample exposed to 2.25 mg/l gold nanorods on day 10. Red arrows show the nanorods in the solution.	46
Figure 30: TEM images of detected gold nanorods in a root sample of a plant exposed to 2.25 mg/l gold nanorods (25 x 69 nm)	48
Figure 31: gold concentrations detected in the exposure solution samples by ICP-MS. (n=3)	50
Figure 32: gold concentration detected in root samples by ICP-MS. (n=3)	51
Figure 33: gold concentration detected in leaf samples by ICP-MS. (n=3)	52
Figure 34: toxicity curve for different concentration gold nanorods on maize plants (n=3)	53
Figure 35: plants transpiration versus time during the experiment	54

CHAPTER I

OVERVIEW

The general goal of this experiment was to investigate the toxic effects of gold nanorods and their uptake in maize (*Zea mays*) plants, including the:

- Determination of the size and shape dependence of gold nanorod uptake by maize plants; and the
- Bioavailability and toxicity of gold nanoparticles to maize plants.

1.2 Introduction

Chemical contamination of soil and water is one of the major environmental issues of the last few decades. Nano-materials are one of the recent problems due to an increasing industrial and medical usage (Salata, 2004) (Zhi Ping Xu, 2006) (Rawat, Singh, Saraf, & Saraf, 2006) (Gonzalez-Melendi, et al., 2008). Their toxicity, fate, and transport became an essential field of study and research in recent years. The definition of a Nano-material (NM) according to the British Standard Institution is any material with one of its dimensions that is less than 100 nm. Nanoparticles are a sub-group of nano-materials with the stricter definition of having at least two dimensions between 1 and 100 nm. (Klaine, et al., 2008) Due to the fast development of nanotechnology in past decades and special physiochemical properties, nano-materials have been utilized in a wide range of applications. The production volume and range of applications are rapidly increasing. Nano-materials provide new properties and capabilities, which were not possible before. Optical devices, electronic, medicine, cosmetic, coating, paints, pigments and molecular diagnostics are some of the major applications that utilize nano-materials. Though

nano-materials provide huge economic and scientific advantages to material science, the negative consequences of emitting massive volumes of NM into the environment are unclear. Figure 1 shows the life cycle of the ten most utilized NM. According to this study, most NMs end up in landfills and soil (Keller, McFerran, Lazareva, & Suh, 2013)

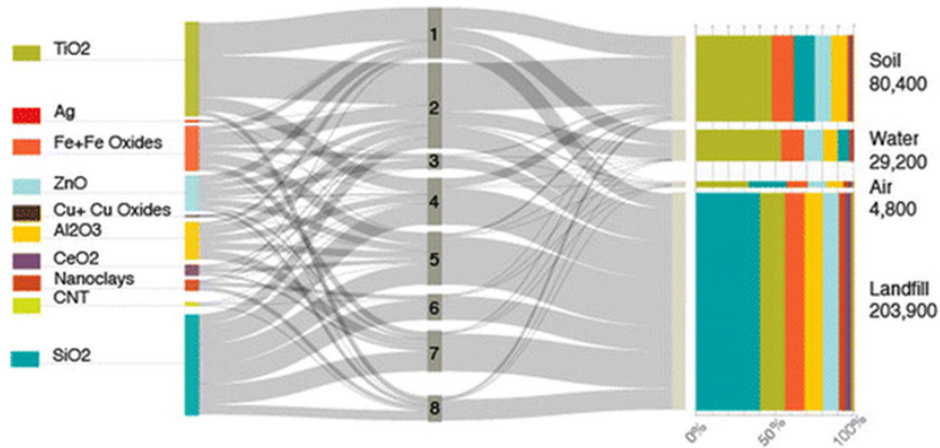


Figure 1: Global flow of ENMs in 2010 (metric tons/ year) from manufacturing to applications and eventual disposal or release into the environment considering the high range of production estimates and releases. Life cycle stages from left (production of ENMs) to right (final disposal or release). (Keller, McFerran, Lazareva, & Suh, 2013)

Utilizing plants for environmental remediation is widely considered as an effective and efficient technological solution called “phytoremediation”. This technology uses plants to remove, degrade, or immobilize contaminants from soil or aquatic systems (Haverkamp, Marshall, & Agterveld, 2007). Phytofiltration refers to a process that specifically removes hazardous heavy metals from contaminated soil and water. (Peer, Baxter, Richards, Freeman, & Murphy, 2006).

According to a study by D.E.Salt, Phytoremediation can reduce environmental toxicity levels through five processes. (Salt, Smith, & Raskin, 1998)

- Phytoextraction removes metal or organics from soil through the use of pollutant-accumulating plants by concentrating them in the harvestable parts;
- Rhizofiltration uses plant roots to absorb pollutants, mainly metals, from water and aqueous waste streams;
- Phytodegradation uses plants and associated microorganisms to degrade organic pollutants;
- Phytostabilization uses plants to reduce the bioavailability of pollutants in the environment;
- Phytovolatilization uses plants to volatilize pollutants
- And also to remove pollutants from air. (Salt, Smith, & Raskin, 1998)

The field of environmental remediation became even more complicated by the recent introduction of engineered nanoparticles (ENPs) from consumer products. The unique properties of this class of nanomaterials have raised concerns of accumulation in environment and the resulting effects on ecosystems, such as the interaction between accumulation of ENPs and plants. The effects of ENPs on various plants and their developmental stages vary. Depending on the concentration, size, and shape of nanoparticles, the effects on plants can be enhancing, inhibiting, or neutral. It has been documented that ENPs can penetrate into the plants and be transported through the plant tissue (Zhai, Walters, Peate, Alvarez, & Schnoor, 2014) (Mamta Kumari) (Corredor, Testillano, Coronado, Gonzalez-Melendi, & Rodrigo Fernandez- Pacheco, 2009) (Zhu, Han, Xiaoa, & Jin b, 2008). Although much research has been done on the behavior of nanomaterials on mammalian and human cells, there have been only a few previous studies on the path, size, and shape dependence and toxic effects of nanoparticles in plants. (Ma, Geiser-Lieb, Dengc, & Kolmakovd, 2010) (Rico, Majumdar, Duarte-Gardea, Peralta-Videa, & Gardea-Torresdey, 2011) (Kráľová, 2012)

Spherical shaped nanoparticles have attracted extra scrutiny due to their special properties. For instance, gold nanospheres have been used in biological electron microscopy. Silver nanorods are

playing an important role in the photography industry. (Murphy & Jana, 2002) Nanorods are essentially the lowest energy form of reduced metal salt. Many methods exist to synthesize gold nanorods such as the Turkvich method, Ferns method, Brust method, microemulsion method, and seeding method. (Murphy, et al., 2008).

Another interesting feature of ENMs is the ability to act as a gene and chemical transporting agent. Studies show that nanoparticles can transport chemicals and genes to plant cells, though the plant cell wall limits this function. (Torney, Trewyn, Lin, & Wang, 2007) ENMs have the potential to revolutionize the field of agriculture. This revolutionary potential, the central importance of nano-materials in modern society, and the knowledge deficit in understanding plant-nanomaterial interaction, all further reinforces the fact that the fate, uptake, and translocation of nanoparticles in the plants is an essential field of study and investigation.

CHAPTER II

LITERATURE REVIEW

Nano-materials are widely used in many different areas of application, such as electronics, cosmetics, industrial, biomedical, and other material applications. The large emission of nano-materials into the environment has motivated increasing concern regarding the effects on the ecosystem, food chain, and human health. This release of engineered nanoparticles into the environment and ecosystems may potentially cause adverse effects. Plants can tolerate a certain amount of natural nanomaterial (Lee, Youn-Joo, Yoon, & Kweon, 2008), but large amounts of ENMs released from a variety of industries could be toxic to the plant profile and possibly threaten the ecosystem. (Daohui & Xing, 2007) (Lee, Youn-Joo, Yoon, & Kweon, 2008) (Atha, et al., 2012) Furthermore the fate, translocation, and toxicity of nano-materials to future generations are still unknown and require further investigation.

Some reports suggest that some dissolved metal ions can precipitate into NPs and accumulate in edible plants. For instance, Au (III) and Ag (I) ions can be reduced in alfalfa seedlings and accumulate as AuNPs and AgNPs. Likewise, Ag (I) and Pt (II) ions convert to NPs in alfalfa and mustard plants. (Rico, Majumdar, Duarte-Gardea, Peralta-Videa, & Gardea-Torresdey, 2011). A study on silver nanoparticle uptake by *Brassica juncea* and *Medicago sativa* reports that in the case of *Brassica juncea*, uptake of NPs was independent of concentration; and for *Medicago sativa*, on the other hand, more particles were uptaken when exposed to higher concentrations of silver nanoparticles (Harris & Bali, 2008). Another study further examined the relationship between nanoparticle concentration and toxicity. In this research, poplars and *Arabidopsis thaliana* were examined for uptake and accumulation of different concentrations of silver NPs,

carbon-coated silver NPs and silver ions. Plants exposed to high concentrations of Ag⁺ ions or AgNPs displayed symptoms of phytotoxicity. Comparing exposed plants and controls showed that at a small range of relatively low concentrations, root growth, fresh plant weight, and evapotranspiration were promoted (enhanced growth). It is also important to note that the silver distribution, accumulation, and localization appeared to differ between species. The results of this research showed that *Arabidopsis* accumulated silver NPs in leaves, while poplars accumulated silver in roots and leaves similarly. Particle size and toxicity were suggested in this experiment to be correlated as well. Poplars and *Arabidopsis thaliana* were more susceptible to silver nanoparticle toxicity as particle sizes decreased (Wang, et al., 2013). Other studies on the toxicity of copper nanoparticles have shown that they inhibit growth in terrestrial plants, such as mung bean (*Phaseolus radiates*) and wheat. Results demonstrated the toxicity and bioavailability of copper. (Lee, Youn-Joo, Yoon, & Kweon, 2008) (Tara Sabo-Attwood, 2012). A further study examined the phytotoxicity of silica nanoparticles (SiNPs) toward *Arabidopsis thaliana* plants as a function of particle size. Concentrations of 50 and 200 nm particles were used in this research, and the study confirmed that the uptake of the nanoparticles by the plants was size-dependent (Schoenfisch, 2012). In a different experiment on pumpkin plants, Hao Zhu et. al. showed that pumpkin plants can uptake magnetic nanoparticles from aqueous medium and accumulated the particles in plant tissues (Zhu, Han, Xiaoa, & Jin b, 2008). In addition, the study suggested that germination and root elongation could be adversely affected by nanoparticles. The experiment was done on *Brassica napus* (rape), *Raphanus sativus* (radish), *Lolium perenne* (ryegrass), *Lactuca sativa* (lettuce), *Zea mays* (corn) and *Cucumis sativus* (cucumber). Results showed that nano-Zn and nano-ZnO affected the germination of ryegrass and corn, respectively, at 2000 mg/L concentration. This concentration of nano-Zn and nano-ZnO also terminated plant root

elongation. (Daohui & Xing, 2007) An experiment on rice plants (*Oryza sativa*) with carbon nanotubes indicated that nanoparticles delayed the flowering and lowered the yield (Sijie Lin, 2009).

High levels of toxic metal accumulation not only posed a potential health risk to humans and animals, but it also reduced crop yield, which potentially caused significant economic damages (Kráľová, 2012).

Phytoremediation is a promising technology, which could potentially combat metal and ENM contamination. Studies have examined numerous potential species and have identified approximately 400 species from 45 plant families with hyperaccumulation characteristics. (Lasat, 2002). Among the species, willow (*Salix viminalis* L.), Indian mustard (*Brassica juncea*), corn (*Zea mays* L.), and sunflower (*Helianthus annuus* L.) are promising candidates that accumulate and tolerate heavy metals (Schmidt, 2003). To further narrow the field of candidates, studies focused on growth rates and biomass production levels. Though some plants are hyperaccumulators, they would not ultimately be effective remediation agents because of their slow growth and low yield. Ultimately, maize (*Zea mays* L.) was able to satisfy all selection criteria. However maize is a food and feed crop, which could demonstrate the hazard of nanoparticle uptake and distribution in the food chain. It also has large biomass yield, high heavy metal tolerance, and is a widely cultivated crop in North America. Maize was shown to be able to effectively accumulate cadmium and lead from contaminated soil (Mojiri, 2011). Corn seeds were inoculated with Nanoceria at 2000 mg/L, reducing germination by 30%. However, subsequent root growth showed a statistically significant increase. Experiments conclusively confirmed that CuO nanoparticles were transported from roots to shoots in maize plants. (Martha L. López-Moreno, 2010) (Li, Li, Zhuang, Zou, & McBride, 2009)

Despite toxicity and other negative concerns, researchers in agri-nanotechnology are interested in nano-materials as a delivery method to plants. Studies show that nanoparticles can transport DNA and chemicals into plants cells. For example, an experiment revealed that mesoporous silica nanoparticles loaded with DNA and its chemical inducer capped with gold nanoparticles were successfully transported to the plant cell and activated gene expression (Torney, Trewyn, Lin, & Wang, 2007). Other studies investigated the uptake and translocation of magnetic nanoparticles in *Cucurbita pepo* and suggested magnetic nanoparticles as a treatment delivery by plants, and as a potential method to attack infection (Gonzalez-Melendi, et al., 2008) (Remya Nair, 2010)

Employing phytoremediation as a contamination treatment method shows promise. However a pre-requisite to successful treatment is better understanding of the behavior and effects of nano-materials within plant systems. This study is designed to investigate the uptake, translocation, bioavailability and toxicity of gold nanorods in maize plants. The findings could be an important contribution to the fields of phytoremediation, agri-nanotechnology, and nanoparticle toxicity.

CHAPTER III

GOALS AND OBJECTIVES

There were five specific objectives and seven hypotheses in this research as follows:

3.1 Objective 1:

To determine the uptake and translocation of gold nanorods by maize plants (*Zea mays*.)

- Hypotheses: Maize plants can uptake gold nanorods from a hydroponic system and translocate them from roots to shoots.

3.2 Objective 2:

To determine the size and concentration dependence of gold nanorod uptake by maize plants.

- Hypotheses: Smaller size nanorods can be uptaken more readily by the plants.
- Hypotheses: Nanorods will be uptaken in greater amounts by plants at higher exposure concentrations.

3.3 Objective 3:

To investigate the bioavailability of gold nanorods to maize in a hydroponic system.

- Hypothesis: Gold nanorods are available for biouptake by maize in hydroponic solution and will be accumulated and detectable in plant leaves and shoots by TEM and ICP-MS.

3.4 Objective 4:

To determine the toxic concentrations (i.e., cessation of transpiration) of gold nanorod to maize.

- Hypothesis: Gold nanorods can be toxic to the maize plants at higher exposure concentrations in hydroponic solution.

3.5 Objective 5:

To study the shape and size change of gold nanorod in maize plants.

- Hypothesis: Gold nanorods will decrease in size in plant tissues after uptake due to dissolution/abrasion in the uptake and translocation process.
- Hypothesis: The morphology of gold nanorods will change during the uptake by maize plants.

CHAPTER IV

METHODOLOGY

The experimental methodology for this research follows in the next few sections. The materials, equipment, samples, experimental procedures, and techniques utilized are as follows.

4.1 Chemicals and Supplies

Information about the chemicals, seeds, growth media and gold nanorods used in this experiment are listed below.

4.1.1 Seed

Sweet corn seeds (*Zea mays*) were purchased from Burpee Garden Products Company (www.burpee.com). Table 1 shows some information on seeds used in these experiments.

Table 1: Corn seed information

Name	Sweet corn
Scientific name	<i>Zea mays</i> var. <i>saccharata</i>
Hybrid	Yellow su- Early Sunglow
Supplier	Burpee Garden Products

4.1.2 Growth solution

Hoagland solution was used as the media and nutrient for hydroponic growth. (Hoagland & Arnon, 1950) Table 2 is the list of contents and the amount used to make a 12 L batch Hoagland solution. A dilute solution of the Hoagland media was utilized (1/10 strength) because it was desirable to keep the ionic strength low and to avoid precipitation of salts from the media.

Table 2: 0.1 strength Hoagland Solution contents for

12 L batch

Contents	Amount added (ml)
1M Ca(NO ₃) ₂ ·4H ₂ O	4.8
2M KNO ₃	3.6
2M NH ₄ H ₂ PO ₄	2.4
Micronutrient	2.4
20 nM Fe-EDTA	2.4
1M MgSO ₄ ·7H ₂ O	1.2
1M NaOH	Until pH= 6.8

4.1.3 Gold nanorod

For this experiment gold nanorods were chosen as the nanoparticles for exposure to maize seedlings because their rod shape can be clearly differentiated in the microscopy imaging and because they are known to be non-reactive in solution (they do not dissolve). For experiment 1, gold nanorod solutions were purchased from Ocean Nano Tech Company (www.oceannanotech.com) in three different sizes. Table 3 contains information of nanorod characteristics and the final concentration used in experiment 1. TEM images taken of nanorod stock solutions in Figure 2 show the nanorod shapes and sizes. Three images were set at the same degree of magnification, and a comparison of the relative size and aggregation of the nanorod particles was visually enabled. The concentration of gold stock solution was not specified in the manufacture information sheet. Therefore the volume of each nanorod was calculated based on its dimension and multiplied by numbers of nanoparticles per milliliter (specified by the manufacture) and the density of pure gold ($1.93 \times 10^{-20} \text{ g/nm}^3$) to get the total mass of nanorods per ml stock solution. 2 mL of stock solution was added to 18 mL Hoagland solution, resulting in the final concentrations given in Table 3.

Table 3: Characteristics of gold nanorods used in experiment 1

Initial	Size (nm)	(#np/mL)	Total Volume (nm ³ /np)	Final Conc. (mg/L)
S	10 x 34	7.6×10^{13}	2410	350
M	20 x 75	1.4×10^{11}	21500	5.8
L	40 x 96	6.95×10^{10}	104000	14

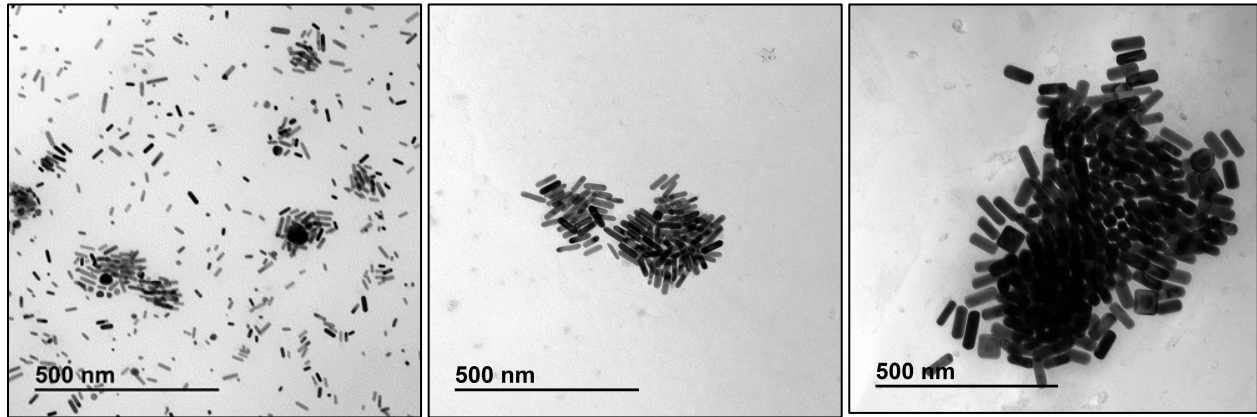


Figure 2: TEM images taken of gold nanorods used in experiment 1. Left) 10x 34 nm. Middle) 20x 75 nm. Right) 40x 96 nm.

The gold nanorod solution for experiment 2 was purchased from Sigma Aldrich Company (www.sigmaaldrich.com) with an absorption wavelength of 650 μm and dispersed in H₂O. Table 4 presents the characteristics and calculated final concentrations for the stock solution concentration of nanorods used in experiment 2. The appearance of the gold nanorods under TEM imaging is shown in figure 3. Both images were taken from the same gold stock solution at different magnifications. As it appears in all TEM images from all four gold solutions, nanorods tended to cluster together in aggregates or it can be result of preparation procedure for TEM.

Table 4: Characteristics of gold nanorods used in experiment 2.

Size (nm)	Volume used (ml/20 ml vial)	(# np/ml)	Conc. (ug/mL)	Total Solution vol (mL)	Total Conc. (mg/L)
25 x 69	1	7.8×10^{10}	45	20	2.25
25 x 69	0.2	1.5×10^{10}	45	20	0.45
25 x 69	0.002	1.5×10^8	45	20	0.0045

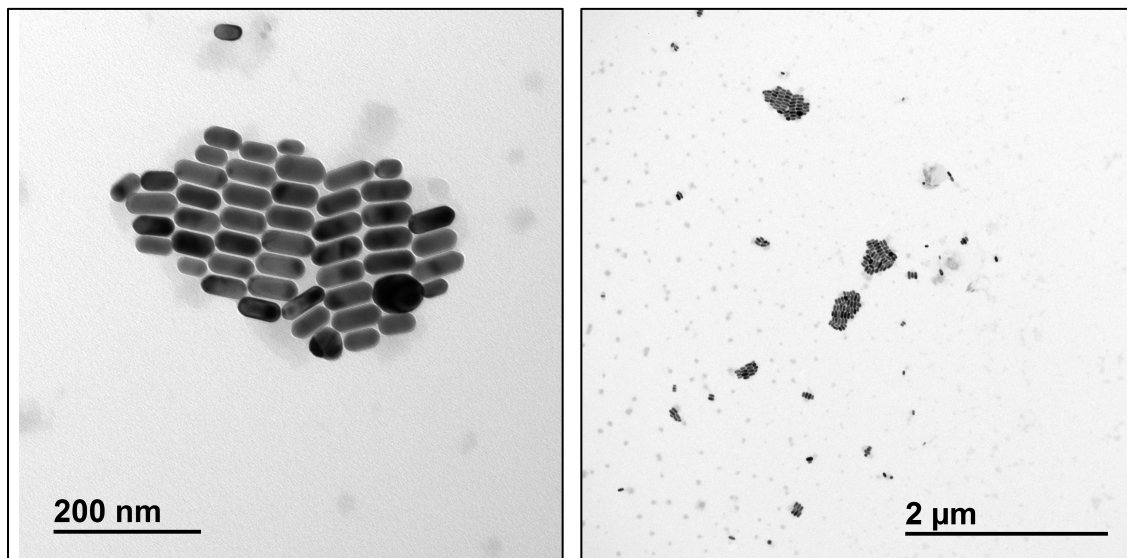


Figure 3: TEM images taken of gold nanorods used in experiment 2. (25 x 69 nm)

4.2 Cultivation and Growth

To investigate the uptake and toxicity of gold nanorods on maize plants in early stages, plants were cultivated from the seed. The methods for seed germination and seedling cultivation are explained in following sections.

4.2.1 Seed Preparation

DI water, dishes, and paper filters were first sterilized in a high-pressure sterilizer (TOMY ES-315) at 120°C for 20 min. Corn seeds were soaked in DI water (Barnstead UV disinfection and

deionized unit) for 5 minutes and rinsed twice with DI water. Then they were soaked in 30 % hydrogen peroxide for 1 minute and rinsed 3 times with DI water. Surface sterilized seeds then were placed on dampened paper in petri dishes and covered with aluminum foil and kept in the dark at 25°C for 7 days. DI water was added every day to keep the papers dampened. Germinated seeds with appropriate roots and stems size were collected for cultivation (Pei, 2013) (Card, 2011). Figures 4 show germinated seeds after 7 days in a petri dish, and the configuration of the cultivation apparatus is shown in figure 5.



Figure 4: Germinated seeds ready to be planted



Figure 5: Germinated seeds planted in 20 mL glass vial.

4.2.2 Plant preparation

Germinated seeds were put in pre-holed caps and 20 mL vials filled with 0.1 strength Hoagland solution and the cap sealed with Parafilm sealing film. All vials were then kept in Percival Plant Growth Chamber with 16/8 day/night cycle at 25°C, 59% RH and with light intensity of 120-180 $\mu\text{mol m}^{-2} \text{s}^{-1}$ for 7 days. 1/10 strength Hoagland solution was added to the vials every other day. On the 7th day, the plants were approximately 11 cm tall from stem base to leaf tip. Healthy green plants of similar height and leaf count were collected for experiments and for exposure to gold nanorods. All experiments were performed in 4 replicates (Three used for transpiration, biomasses and ICP-MS and one for TEM).

4.3 Sampling

Four replicates of plants were sacrificed on each time point for dry and wet biomass measurements and TEM and ICP-MS analysis. The total Hoagland solution volume added to each vial was measured which indicated the water replaced by plant transpiration and evaporation on a daily basis. This volume was used to calculate total cumulative transpiration during the course of the experiment. Also the appearance and health of the plants were observed carefully, and photos were taken for comparison.

4.3.1 Sampling for TEM

One plant from each group was randomly picked for TEM imaging. For this purpose, samples were divided into root and shoot parts with sharp blade. Each part was chopped into cross section

to less than 1 mm³ under the surface of 1/2 strength Karnovsky's fixative solution. Samples were then kept in the Karnovsky's solution at 4°C until further processing.

4.3.2 TEM Preparation method

Plant tissue samples were kept in ½ strength Karnovsky solution at 4°C. To prepare samples for TEM, Karnovsky fixative solution was taken out of the vials and the procedure below followed:

Table 5: TEM preparation procedure ((Russell, 1999) modified by Katherine Walter)

Treatment	Frequency and Time
0.1M Cacodylate Buffer	3 changes in 30 min
1% OsO ₄ in 0.1 M Cacodylate	1 hour
0.1M Cacodylate Buffer	3 changes in an hour
DI H ₂ O rinse	1 min
2.5%Uranyl Acetate	1 hour
Different concentrations of Acetone and Propylene Oxide	1 hour each
1 part Acetone, 1 part Propylene Oxide	30 min
Propylene Oxide	2 changes in an hour
Different Concentrations of Propylene Oxide and Spurr's	1 hour each
100% Spurr's	5 hours

One or two pieces of each sample tissue was then embedded in fresh Spurr's in a flat embedment mold and placed in the 70°C oven for 24 hours. After microtomy and staining with uranyl acetate and lead, they were examined with JEM- 1230 Electron Microscope. Figure 6 is a photo of JOEL JEM Electron Microscopy used for TEM in this experiment.



Figure 6: JOEL JEM- 1230 Electron Microscope used for TEM imaging

4.3.3 Sampling for ICP-MS

The rest of the maize plants from each group were prepared for ICP-MS testing. These samples were divided into roots and shoot parts by a sharp blade. Each part was weighed and placed in separate vials. All samples were then oven dried at 60°C for 48 hours and weighed again afterwards. All dried samples were kept at 4°C until further processing.

4.3.4 ICP-MS preparation method

The following procedures were utilized to prepare all solutions and plant samples for ICP-MS analysis of total gold concentrations.

4.3.4.1 Filtered Solution Samples

Filtered solutions were tested to investigate if any dissolution of gold nanorods occurred in the solution during the exposure period. First, to reduce any contamination from previous experiments, clean Teflon beakers were filled with a mixture of HNO₃ and HCl and kept on the

hot plate over night at 90°C to remove any residuals . Beakers then were rinsed with milli-Q water and dried.

Three replicates of each solution samples were chosen for ICP-MS. Also three recovery samples were added (no sample added). Solutions were first filtered through a membrane centrifuge in Amicon Ultra-4 3K Filter (Merck Millipore Ltd.) on 10000 rps for 20 minutes to remove gold nanoparticles. Gold ions presumably remained in the filtered solution. 1.0 mL of filtered solutions were added to the Teflon beakers and dried for 3 hours at 90°C on hot plates. Then 3 mL of Aqua Regia solution (freshly mixed nitric acid and hydrochloric acid 3:1) was added to dissolve the gold metal. Sample vials were kept on a 90°C hotplate for 6 hours, then dried for 4 more hours on the hot plate. On the last step, dried samples were dissolved in 3 mL 2% HNO₃ and 2% HCl solution. Also 100 µL of 1.64 µg/L of RE solution was added as an internal standard.

After preparation, samples were added to plastic tubes, and the ICP-MS instrument was used to analyze the gold ion concentrations in the samples.

4.3.4.2 Leaf and Root Samples

Dried Leaf and root samples were ground up with mortal and pestle. Then they were weighed and were transferred to clean Teflon vials. Because the amount of gold expected may be lower than detectable limits, 0.45 mL of 1.37 ppm Au stock solution was added to all samples. Samples then were digested in 1 mL hydrogen peroxide and 3 mL nitric acid on the hotplate at 70 C overnight. 6 mL of HCl then was added to each sample and heated for an additional 4 hours. 0.25 mL RE solution was added to 30 mL clean bottles as an internal standard and weighed. 10 mL of 2% HNO₃ 2% HCL mixture was added to each sample, then transferred to the 30 mL bottles, and

weighed again to get the final volume of the solution. Finally, samples were filtered with Millex syringe- driven filter units to separate any particles in the solutions, and filtered samples were transferred to plastic tubes for the test.

4.3.4.3 Unfiltered Solution Samples

For preparing these samples, the same procedures as filtered samples were followed except that samples were not filtered through the centrifuge.

All samples were analyzed by Thermo Scientific X-Series 2 ICP-MS instrument, shown in figure 7.

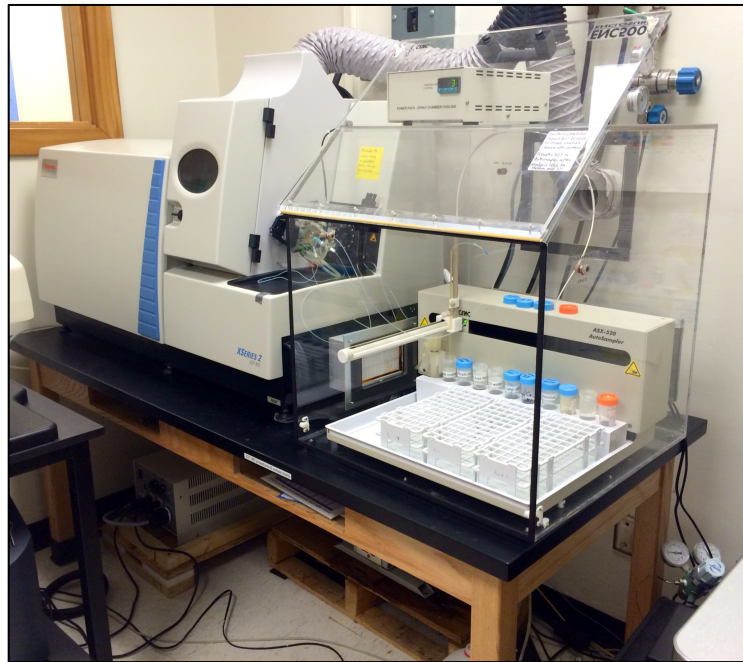


Figure 7: Thermo Scientific ICP-MS instrument used for analyzing data on this experiment

CHAPTER V

EXPERIMENTAL PROCEDURE

The experimental procedure is outlined in the following sections. These experiments were designed to investigate the uptake, toxicity and bioavailability of gold nanorods in maize plants following hydroponic exposures.

5.1 Experiment 1

This experiment was designed to study the uptake of different size gold nanorods at high concentrations, which might elicit a toxic response. After germinating sterilized seeds and cultivating them in the growth chamber, similar looking plants were picked for nanorod exposure. These plants were hydroponically exposed to similar doses of commercial non-coated gold nanorods of various sizes. Gold nanorod dimensions (sizes) used in this experiment were 10x34 nm, 20x75 nm, and 40x96 nm. These dimensions are designated small, medium, and large respectively. Each group of 12 maize plants was exposed to one particular size of gold nanorods. 2 mL of gold stock solution of each size was added to a vial and filled to 20 mL with 0.1 strength Hoagland solution which resulted in 350 mg/L (10x 34 nm), 5.8 mg/L (20 x 75 nm) and 14 mg/L (40 x 96 nm) final concentrations. Control plants also were treated by the same procedures and blank solutions without nanorods. All plants were kept in the growth chamber at 25°C and 16/8 day/night cycle and 59% RH for 10 days. 10% strength Hoagland solution was added to each vial every other day. The amount of solution added was recorded as a measurement of plant transpiration. Four replicates of each experiment group were sacrificed on every time point. The samples, 12 total at each time point (three nanorod sizes x four replicates), were weighed before

and after being oven dried, and then prepared for ICP-MS analysis. Also one sample for each time point was prepared for TEM imaging.

5.2 Experiment 2

This experiment was designed to investigate the effects of various low concentrations of the same size gold nanorods, and their uptake by maize plants. The nanorod solution that had the most toxic effect on plant growth in experiment 1 was group M, 25x69nm nanorods. This size was selected for experiment 2. After cultivation and growth, similar plants were chosen, and maize plants were exposed to 4.5×10^{-3} , 0.45, and 2.25 mg/L gold nanorods. Vials were then filled with 0.1 strength Hoagland solution up to 20 ml. Exposed plants were kept in the growth chamber at a temperature of 25°C and with a 16/8 day/night cycle and 59% humidity for 10 days. The volume of Hoagland solution added to each vial every other day was recorded as a measurement of transpiration. Blank control plants were treated the same except they were not exposed to nanorods. Four replicates of each sample were taken on day 5 and 10 during the experiment, three weighed for wet and dry biomass, then prepared for ICP-MS and one was prepared for TEM imaging.

CHAPTER VI

RESULTS AND DISCUSSION

During and following each 10-day experiment, observations and measurements were examined and compiled as recorded in this chapter. The first experiment was to discover the threshold of toxicity of the gold nanorods and the effect (if any) of various sizes of nanorods on that toxicity. The second experiment was to investigate the effect of concentration on the uptake, translocation and toxicity at much lower concentrations. Samples were analyzed with TEM microscopy in both experiments and by ICP-MS in only experiment 2.

6.1 Experiment 1

This experiment was focused on the toxicity of various sizes of gold nanorods to maize plants exposed in hydroponic solutions to three sizes of nanorods at high concentration.

6.1.1 Appearance

Maize plants health was carefully studied during the experiment. As figures 8, 9 and 10 show, all exposed plant leaves started to turn yellow on day 2 after exposure. Transpirations were low and growth insignificant, and roots were stained purple. On day 6, exposed plants leaves and stems turned brown and withered (Figure 10). All exposed plants were close to death on day 10 and their roots were mushy and dark. In contrast, transpiration was normal in the control plants. Their roots were clear and healthy and they appeared green and growing through day 10. (Figure 10)

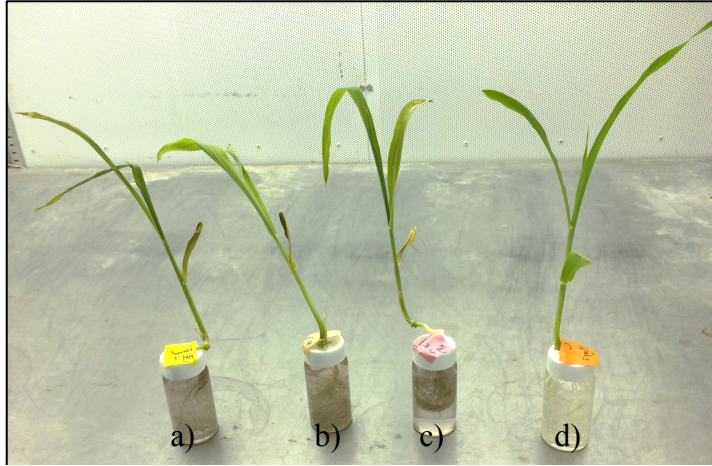


Figure 8: Maize plants exposed to a) 350 mg/L. b) 5.8 mg/L. c) 14 mg/L gold nanorods. d) control. On day 2

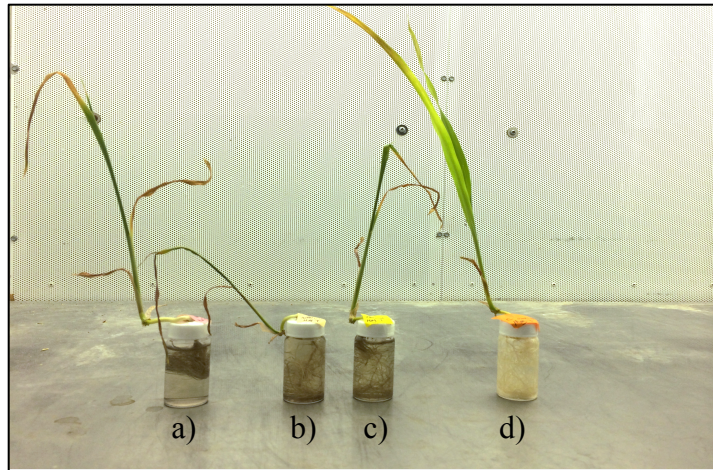


Figure 9: Maize plants exposed to a) 350 mg/L, b) 5.8 mg/L, c) 14 mg/L gold nanorods, d) control, on day 6

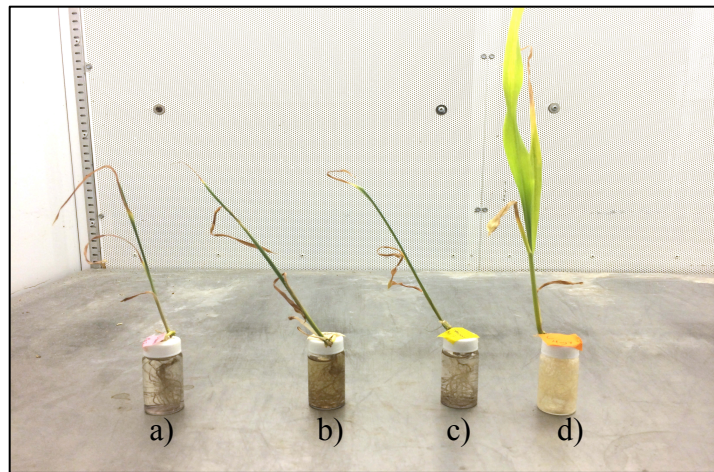


Figure 8: Maize plants exposed to a) 350 mg/l, b) 5.8 mg/L, c) 14 mg/L gold nanorods, d) control, on day 10

6.1.2 Transpiration

Total Hoagland solution volume added to each plant was considered as a measurement of plant transpiration. Transpiration was quantified by summing the solution volume added to exposed plants, and it was compared to the volume added to control plants. As Figure 11 indicates, control plants cumulatively transpired 15 ml of solution on average through day 10. By comparison, in exposed plants, uptake was less than one third of the controls. All three size groups showed statistical significantly lower transpiration. Maize plants exposed to the lowest concentration of nanorods (5.8 mg/L) had the lowest transpiration (3.5 ml) than other exposed plants. However, the differences were not significant at the $p=0.05$ significance level (two-tailed T-test).

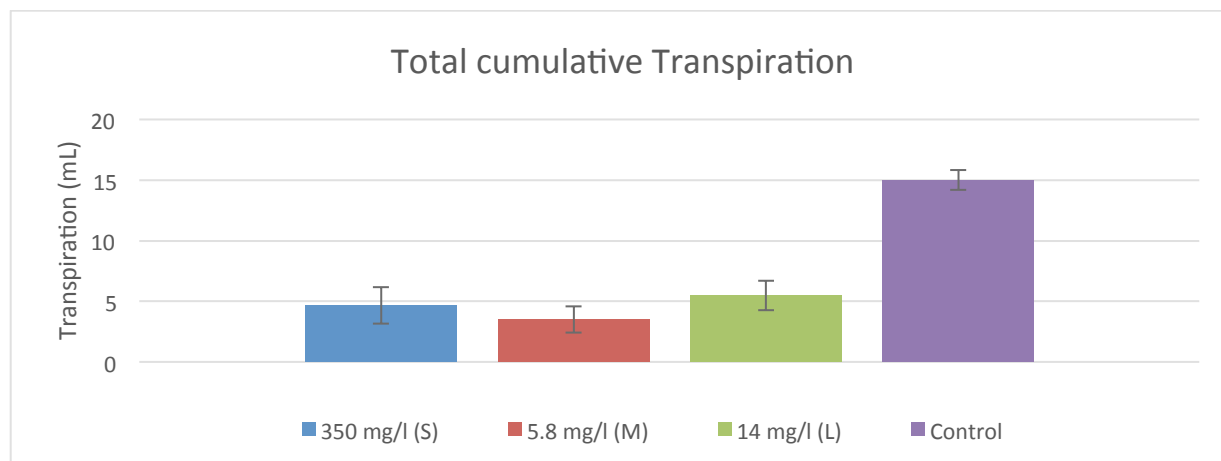


Figure 9: Cumulative transpiration of maize plants exposed to different size gold nanorods and controls in 10 days experiment (n=3)

The transpiration data shows that maize plants were unable to uptake water from hydroponic solution contaminated with gold nanorods at these high concentrations. The mechanism of toxic effect is likely to be centered in the root system. Stained roots during the experiment can be evidence that the reduced transpiration rates may be the result of nanorods accumulating in the roots or on the surface of the roots, thus blocking uptake pathways. Lower transpiration and death of the plants by day 10 are additional indications of toxic effects of gold nanorods to maize plants.

6.1.3 Growth

Fresh samples taken at each time point were weighed and recorded as indicators of growth.

Figure 12 bar graph displays the wet biomass of exposed plants on day 2, 6, and 10 compared to control plants. The increasing trend of control plant biomass shows the growth that is to be expected of healthy plants. The exposed groups did not show significant growth between day 2 and day 6, and they displayed negative growth on day 10, which is a result of water content lost.

The exposed plants wet biomass were approximately 1/3 that of the control plants, which is consistent with transpiration measurements.

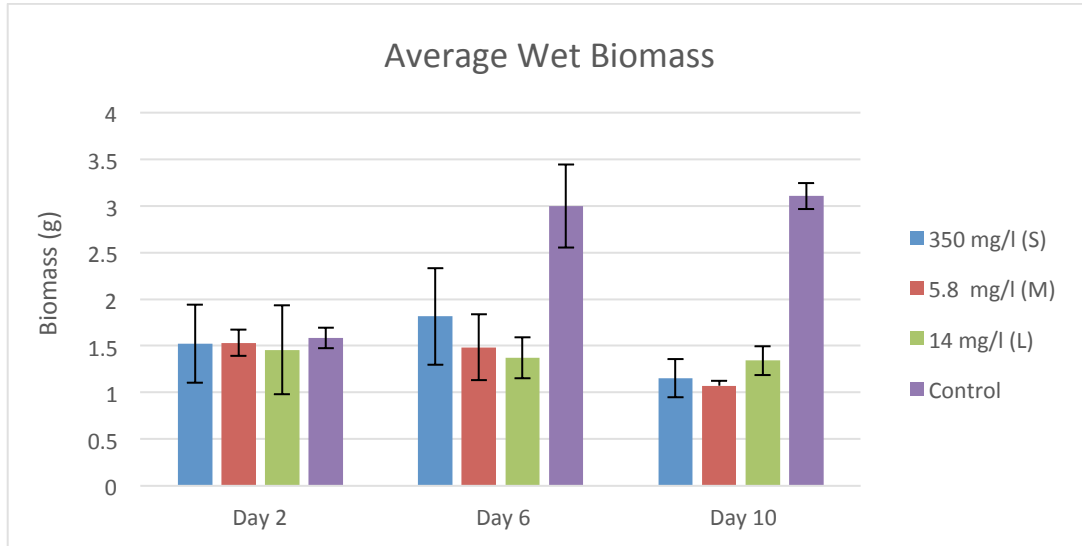


Figure 10: Wet biomass of maize plants exposed to different size gold nanorods on each time point. (n=3)

After the wet biomass measurements were taken, samples were oven dried at 60 °C for 48 hours. Dried samples then were weighed and recorded. This dry biomass measurement excludes the water content in the plants and can be a good indicator of plant growth. Figure 13 shows that maize plants in all groups were growing during the 10-day experiment. However exposed plants showed smaller gains in dry biomass, when compared to the control group indicating some stress or toxicity. The medium size group (exposed to 5.8 mg/L) showed the lowest gains among exposed groups. The results are not statistically significant, but suggest that the particular size 20x75nm with concentration of 5.8 mg/l have additional inhibitory effects on the plants compared to other nanorod sizes.

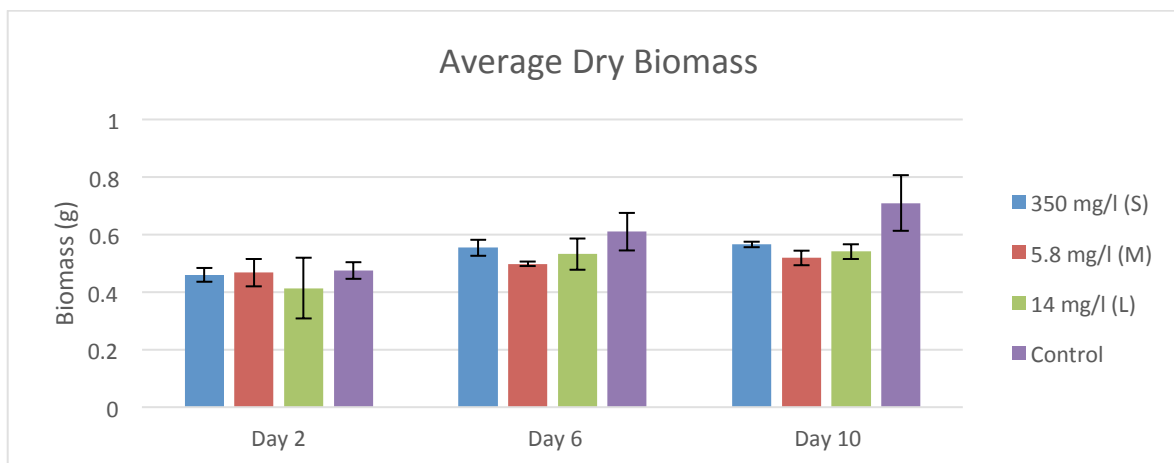


Figure 11: Dry biomass of maize plants exposed to different size gold nanorods on each time point. (n=3)

In this experiment, transpiration and wet and dry biomass analysis showed similar trends. It is also important to state that the nanorod exposures were fatal to the plants by the end of the experiment for all three nanorod sizes (day 10). The growth inhibition was not statistically significant in dry biomass measurement, and the effect was far less pronounced than for transpiration and wet biomass measurements. From visually observing the roots, it was evident that solution uptake (transpiration) was hindered by the presence of nanorods, and that growth inhibition may be a secondary effect. This conclusion supports the hypothesis that nanorod have toxic effects that begins in the roots and affects nutrient uptake mechanisms.

6.1.4 TEM Results

Transmission Electron Microscopy was used to visually search for possible uptaken nanoparticles in the plant tissue cells. In this microscopy technique, a beam of electrons passes through the extra-thin layer of specimen, generating a focused and magnified image of the interaction between electrons and the specimen.

Samples taken on day 10 from maize plants exposed to 20 x 75 nm AuNPs (5.8 mg/L) were prepared through the TEM Preparation Method (sections 5.3.1 and 5.3.2) and examined with JOEL JEL-1230 Electron Microscope (Figure 6). Images below show the TEM imaging results.

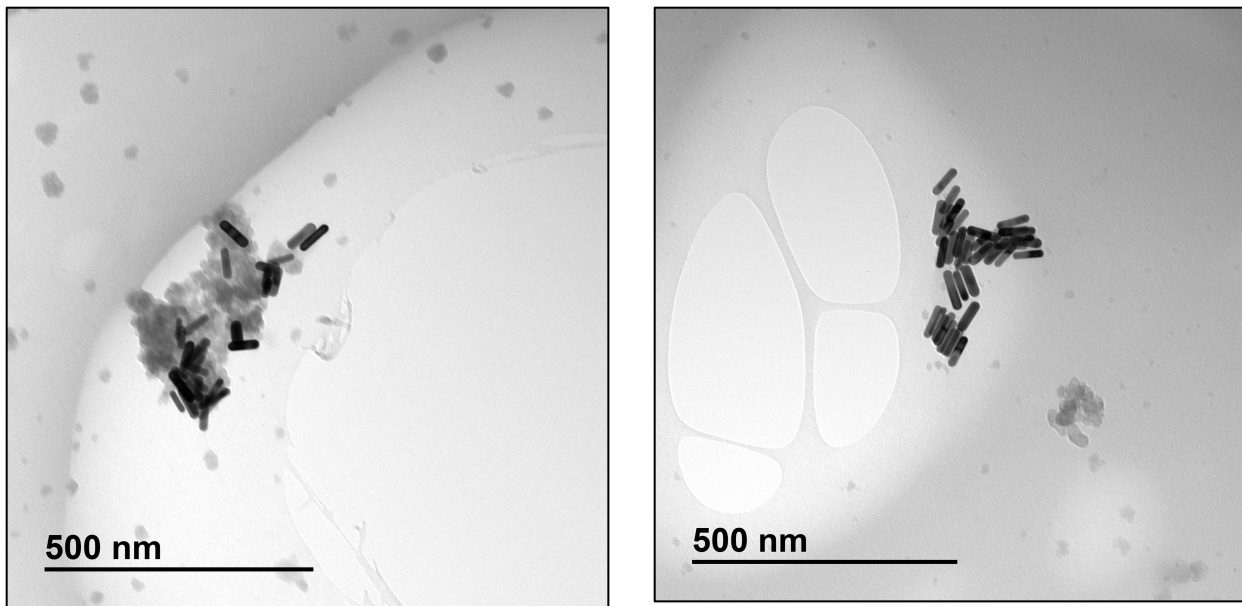


Figure 12: TEM images taken of Hoagland solution exposed to medium size (20 x 75) gold nanorods (5.8 mg/L) on day 10

Figure 14 shows TEM micrographs of the Hoagland solution containing 20 x 75 nm Au nanorods with a concentration of 5.8 mg/L after 10 days exposure. In this Figure, nanorods are clustered together with other particles in the solution. The Au-nanorods are more electron dense and are visible as black rods in Figure 14. Root and leaf samples were also examined by TEM and Figures 15-20 display the nanorods that were detected in maize plant tissues (red arrows). Nanorods were not detected in any control plant tissue samples and an equal amount of scanning effort was performed in both cases. In these images of exposed plant tissues, nanorods were not detected within any specific cell location or organelle, and therefore uptake into plant cells was not observed based these images. Most of the detected nanorods were located in the root cells.

Their rod-shape and high electron density differentiated them from other black dark spots in the cells (they can be a result of preparing the samples for TEM imaging). Rod shaped dense particles were not observed in control plant samples.

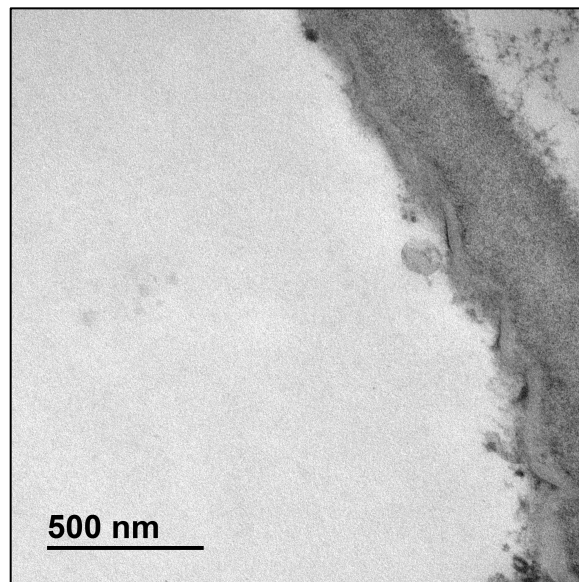
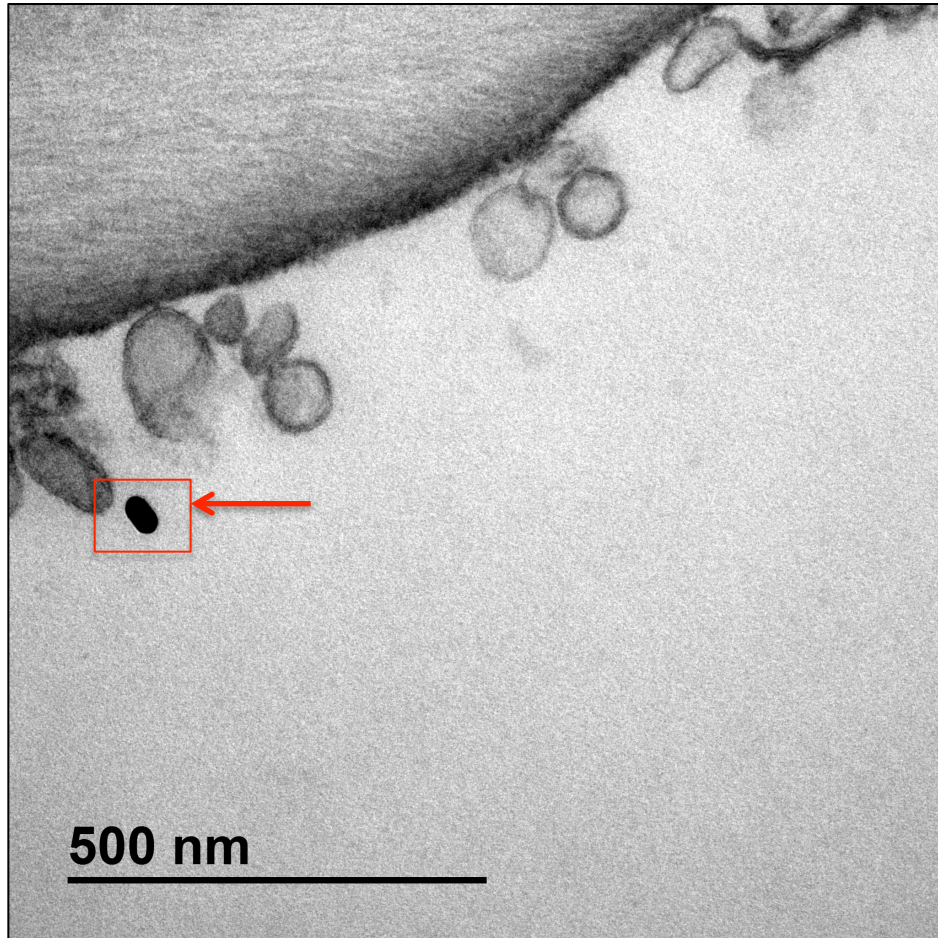


Figure 13: Top) A gold nanorod in a leaf tissue sample from a maize plants exposed to 5.8 mg/L/ The size appears to be consistent with the nanorods used in the experiment, 20 x 75 nm. Bottom) control plants tissue sample with no nanorod detected

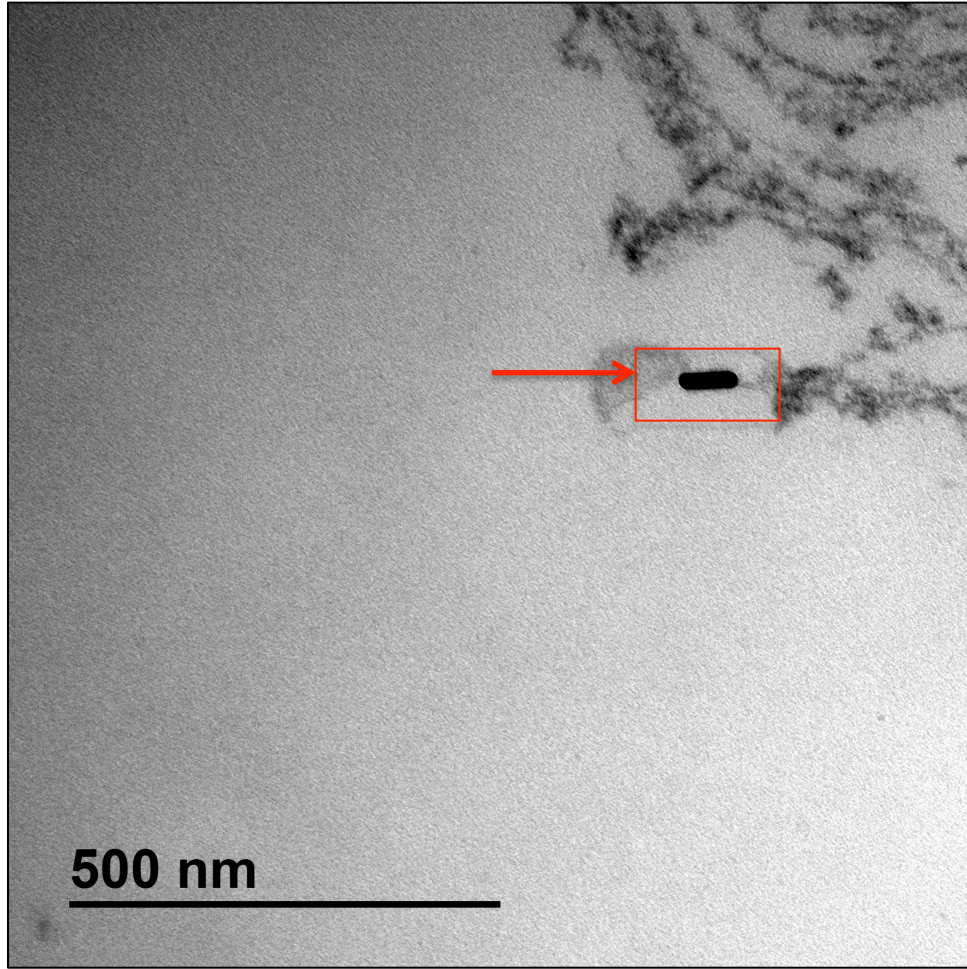


Figure 14: A gold nanorod in a root tissue sample from a maize plant exposed to 5.8 mg/L gold nanorods, 20 x 75 nm

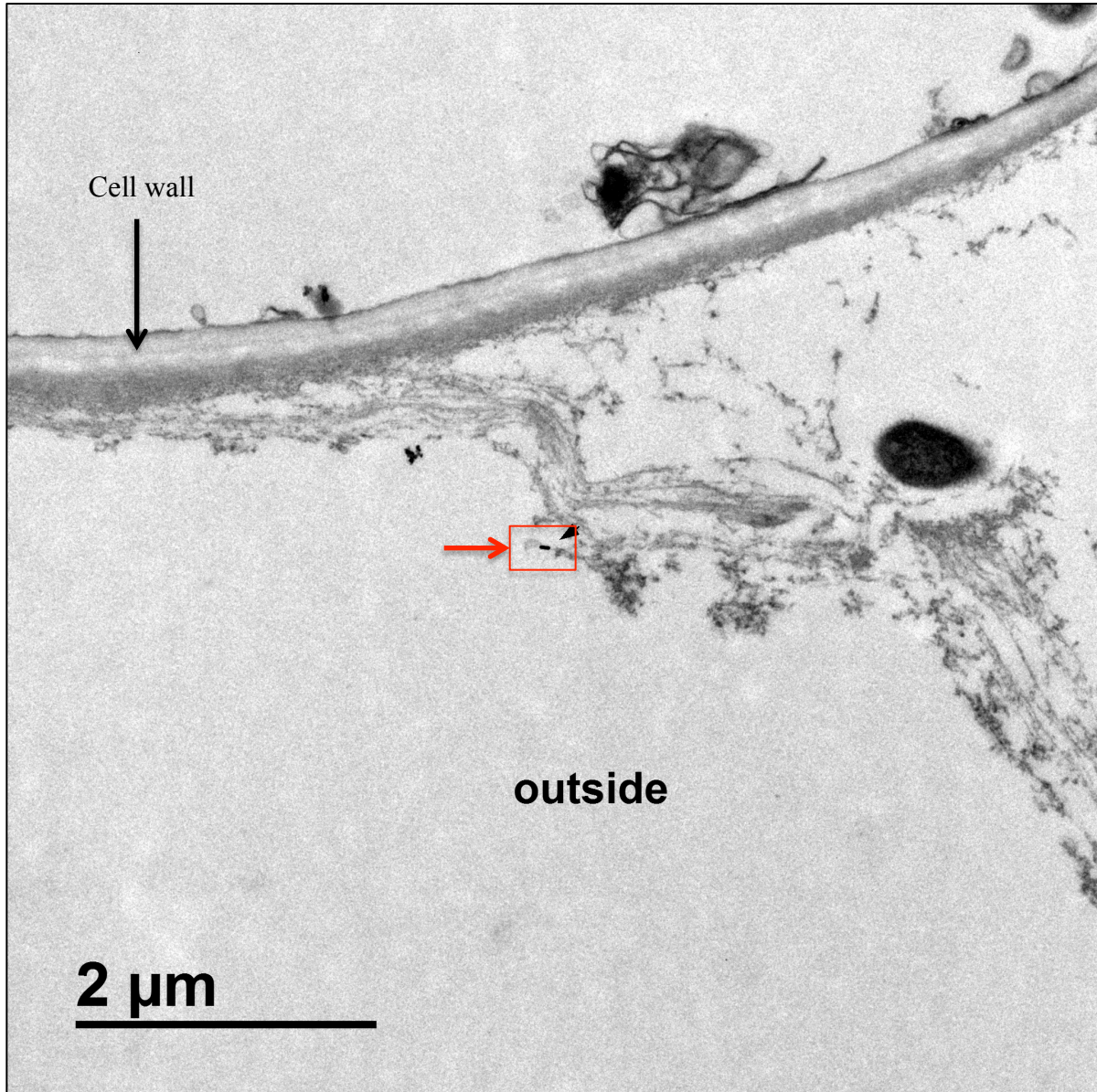


Figure 15: A gold nanorod was detected in this root tissue sample from a maize plant exposed to 5.8 mg/L gold nanorods, 20 x 75 nm. (Outside of the cell)

Figure 17 (above) shows a gold nanorod detected near the cell wall, outside of the root cell. And in figure 18, a gold nanorod in an intercellular space of the root tissue is shown. In both images, nanorods are perfectly in rod shape and very electron dense. Other black dots in the image are not nanorods due to their shape and electron density.

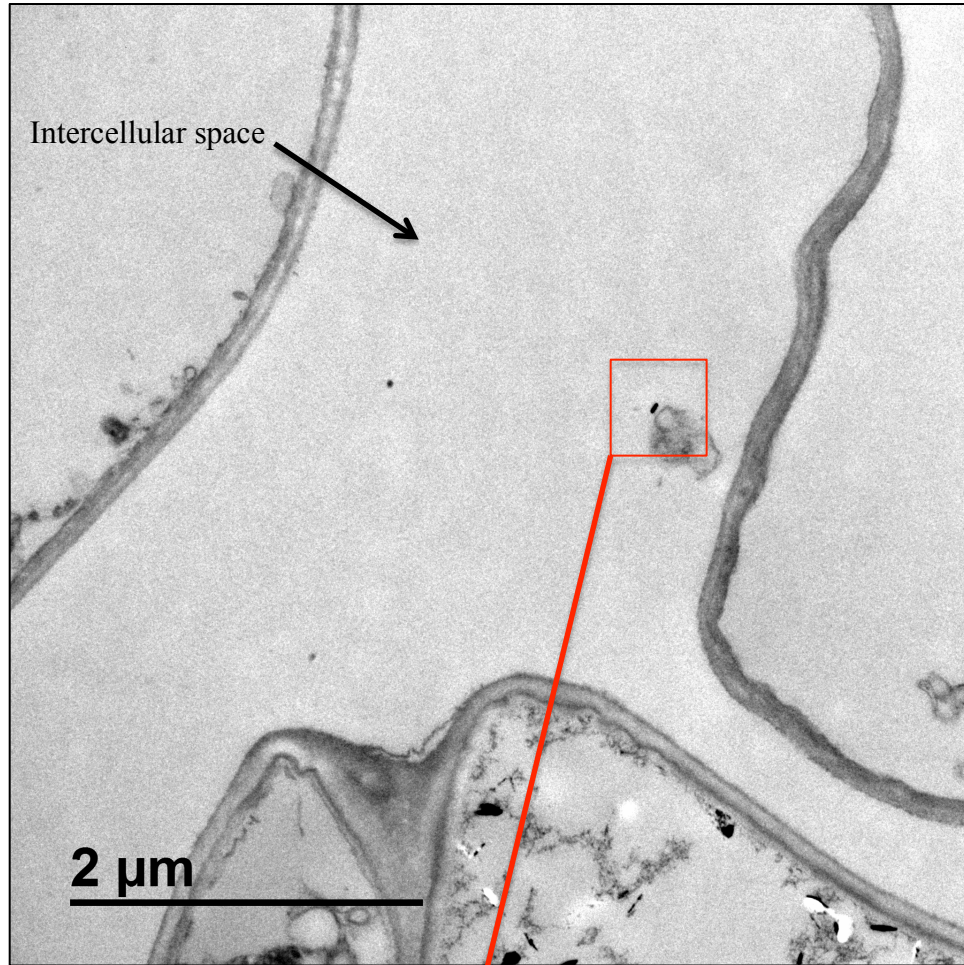
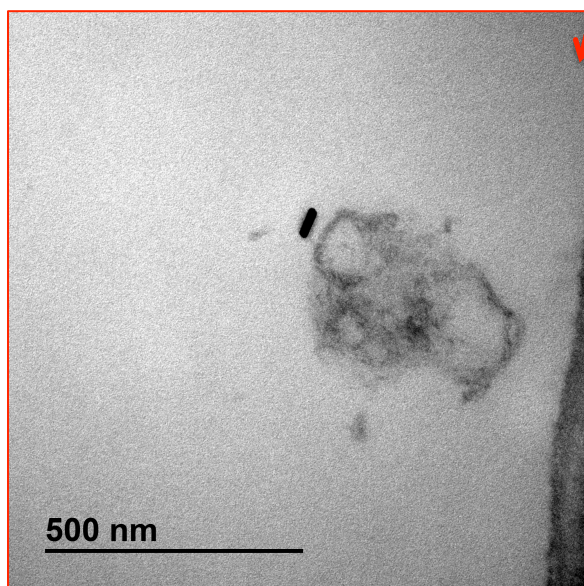


Figure 16: A gold nanorod was detected in this root tissue sample from a maize plants exposed to 5.8 mg/L of gold nanorods, 20 x 75 nm



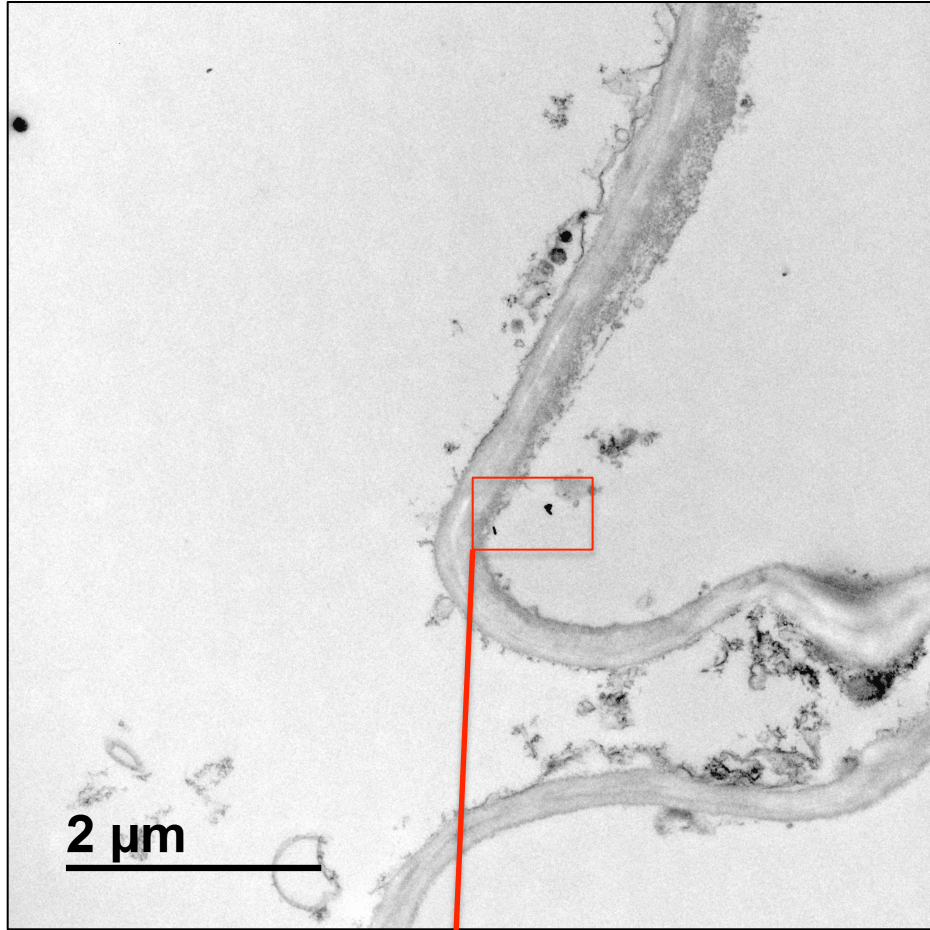
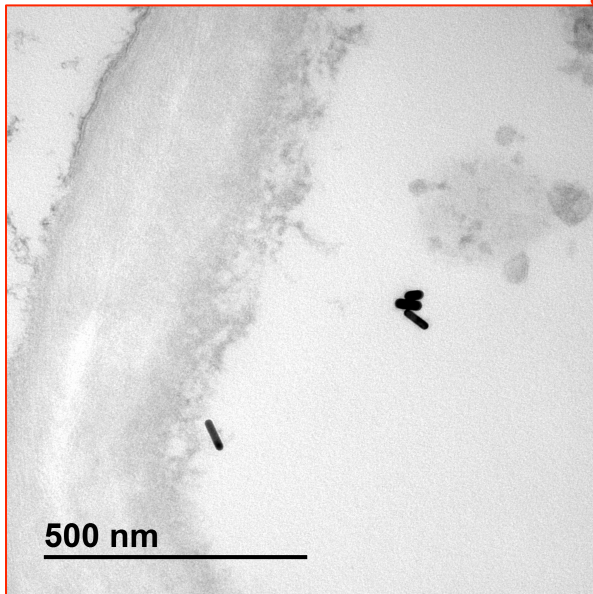


Figure 17: A gold nanorod was detected on this root tissue sample from a maize plants exposed to 5.8 mg/L of gold nanorods, 20 x 75 nm



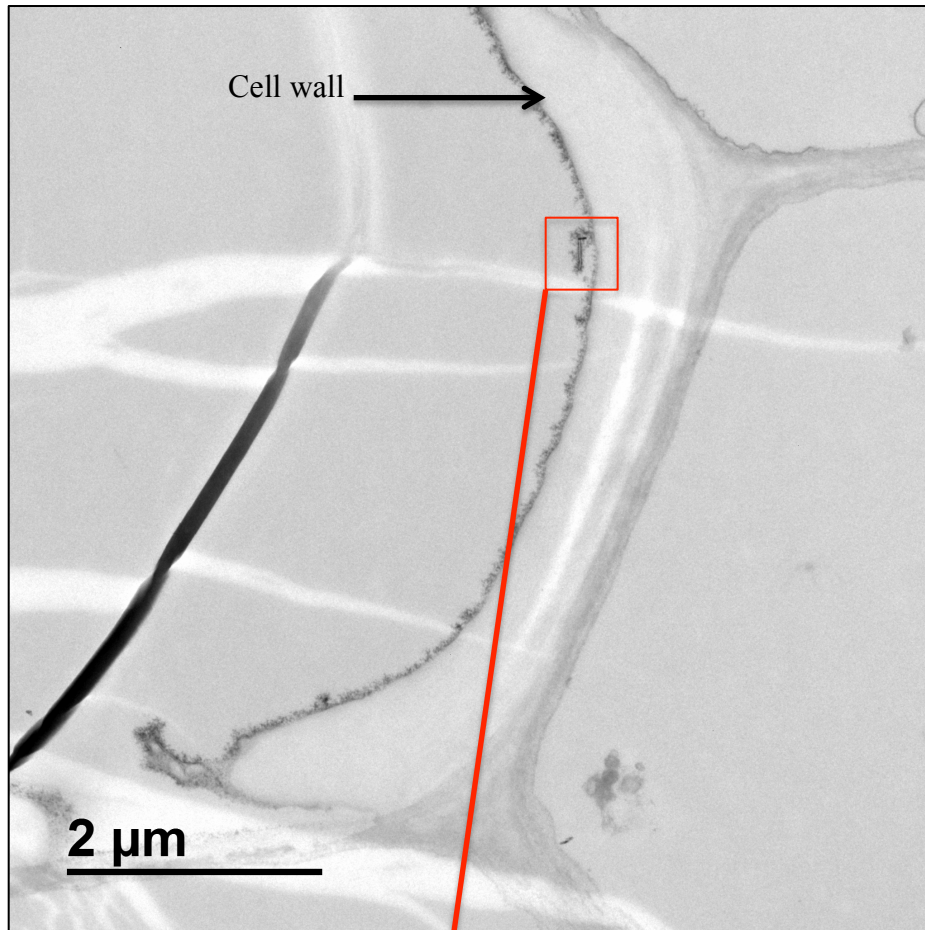
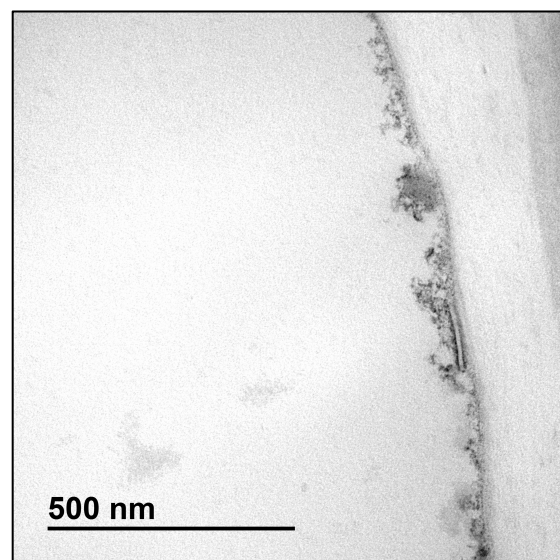
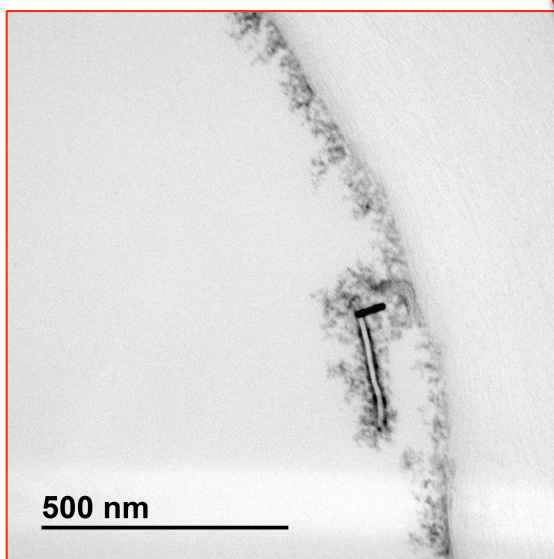


Figure 18: Top and bottom left) A gold nanorod was detected on this root tissue sample from a maize plants exposed to 5.8 Mg/L of gold nanorods, 20 x 75 nm. Bottom right) Tissue sample from control plants without any visible nanorods



Figures 19 and 20 display the nanorods, which were detected by TEM in the root samples of exposed plants and controls. Nanorods in these images were detected close to the root cell walls. In Figure 19, three nano-particles are seen in a cluster. In Figure 20, a single nanorod is stuck to an unidentified long-rod shaped organelle. The same organelle was detected in control plants, but the root tissue of the control did not show any nanorods present. Nanorods detected in or attached to the leaf and root cells were roughly of the same size and shape as the stock solution (20 x 75 nm). However, sometimes the nanorod image may not have been oriented exactly planar with the viewing image and, hence, the nanorod may appear slightly shorter than 75 nm.

Experiment 1 investigated the uptake of gold nanorods of various sizes by maize plants at high concentrations to determine the threshold concentration for toxicity. Seedlings were exposed to non-coated water-soluble gold nanorods in three different sizes through hydroponic system at high concentrations. The transpiration, wet and dry biomasses were measured to compare the growth and uptake of exposed plants to healthy control ones. Plant root and leaf tissues also were examined by TEM. Results showed that maize plants exposed to all three different sizes nanorods were close to death after 10 days (figures 8-10). Not long after exposure, plant roots were stained purple, and after 10 days, they were mushy and not healthy enough to uptake water and nutrition. Exposed plants had considerably lower transpiration and wet biomass than control plants (figures 11-12). Likewise dry biomass was reduced (figure 13), but the effect was less pronounced than that of transpiration and wet biomass. TEM images of root and leaf tissues demonstrated that the maize plants were able to uptake nanorods into the leaf tissue, but few nanorods were detected in shoots. Although the effects of size and concentrations of gold nanorods on amount of uptake is undetermined by this experiment but gold nanorods in all three sizes and high concentrations interfered with water uptake mechanism and growth, which caused

death after 10 days. (Navarro, et al., 2008) The reduced transpiration and water content, which eventually proved fatal to exposed plants, was most likely a toxic effect by physically hindering the root system. The high concentration of nanorods in the hydroponic system most probably interrupted the apoplastic pathway through the root system and inhibited water uptake, which caused the toxic effect. The biomass growth and transpiration of plants exposed to different size particles were not significantly different. Therefore a size-dependent toxicity of nanorods by maize plants was not suggested by this experiment (Asli & Neumann, 2009). The agglomeration of nanorods in the cell tissues was observed by electron- microscopy. The TEM images of samples from plants exposed to 20 x 75 nm (5.8 mg/l) nanorods demonstrated that maize plants were able to uptake nanorods from the hydroponic system, though very few particles were detected in plant tissues after a few hours of searching the TEM fields. Most of the detected nanorods were concentrated in the root tissue. This observation supports the hypothesis that nanorods in the root cells physically hindered nutrient uptake. TEM images proved that maize plants were capable of uptaking gold particles as large as 20 x 75 nm and accumulated them in roots and few observations in the leaf cell. All detected nanorods were in the same shape and size of their stock solution (Figure 2). Therefore, the morphology of the nanoparticles was not changed in size or shape during the uptake process. The translocation factor and mass of gold nanorods from root to leaf was very low in this experiment, which reinforces the hypothesis that gold nanorods blocked the uptake pathways in the root. Very few studies have focused on the uptake mechanism and pathways through the plants. Possible hypotheses are endocytosis, binding to carrier proteins, transport through intercellular plasmodesmata, bacteria, and electrical charge attraction. (Ma & Lin, 2013) (Onelli, Prescianotto-Baschong, Caccianiga, & Moscatelli, 2008)_(Zhai, Walters, Peate, Alvarez, & Schnoor, 2014) (Rico, Majumdar, Duarte-Gardea,

Peralta-Videa, & Gardea-Torresdey, 2011). This experiment did not focus on the exact mechanism of uptake, which is still unclear and requires further investigation but one possible hypothesis for this experiment is disfunction root cells. Roots got mushy and brown during the exposure and they were not uptaking water. It is possible that sick root cells were not functioning at the end of the exposure due to the stress from being exposed to high concentrations of nanorods and they became permeable to rods, which resulted in unwanted uptake of nanorods.

6.2 Experiment 2

Experiment 2 focused on low concentrations (sub-lethal, chronic exposure) of the same size gold nanorods and their uptake by maize plants. Its purpose was to determine the effect of concentration on the uptake of nanoparticles, translocation, transpiration, and growth.

6.2.1 Appearance

Maize plants were closely observed for any change in their appearance during the 10-day experiment. As figures 21 and 22 show, plants exposed to all three concentrations of nanorods appeared to be healthy specimens. Leaves and roots were green and consistent in color with that of the control plants.

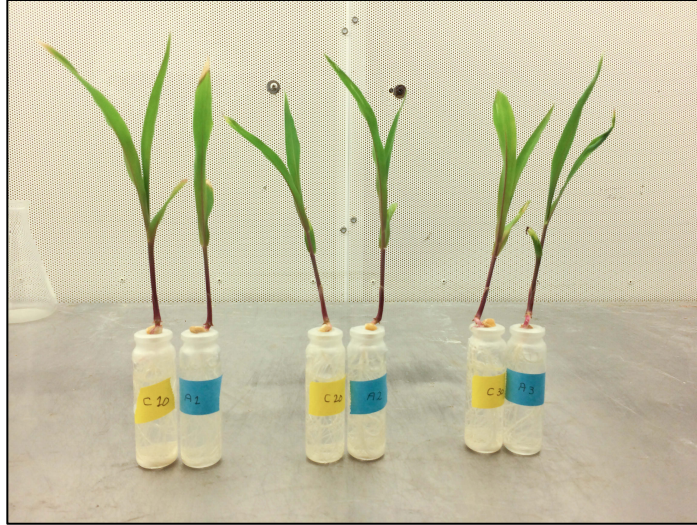


Figure 19: Maize plants exposed to gold nanorods on day 5. Blue label) plants exposed to 2.25 mg/L. Yellow label) control plants

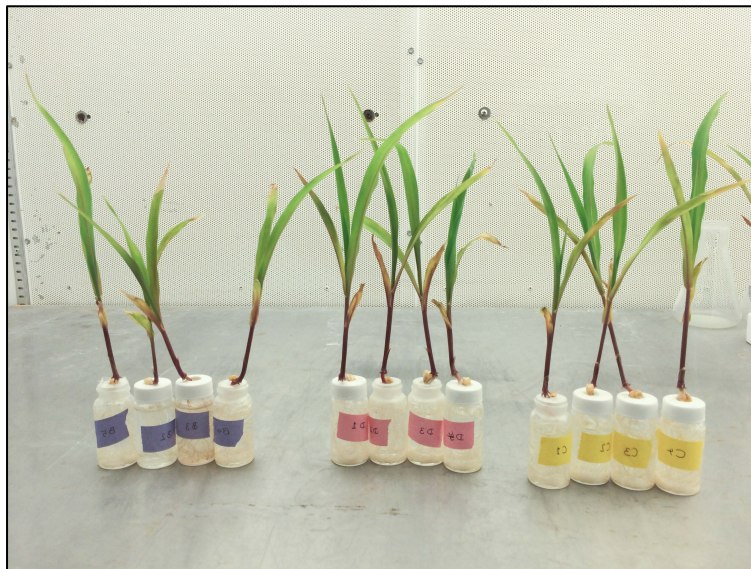


Figure 20: Maize plants exposed to gold nanorods on day 5. Left) 0.45 mg/L. Middle) 4.5×10^{-3} mg/L. Right) control plants

On day 10, the height of exposed shoots appeared to be shorter than that of the controls. However, plant vigor remained indistinguishable. Roots were still healthy and functional with normal color and growth. Exposure hydroponic solutions were clear, and uptake of solution by

all plants was normal compared to that of controls. Figures 23 and 24 show the appearance of the plants after 10 days.

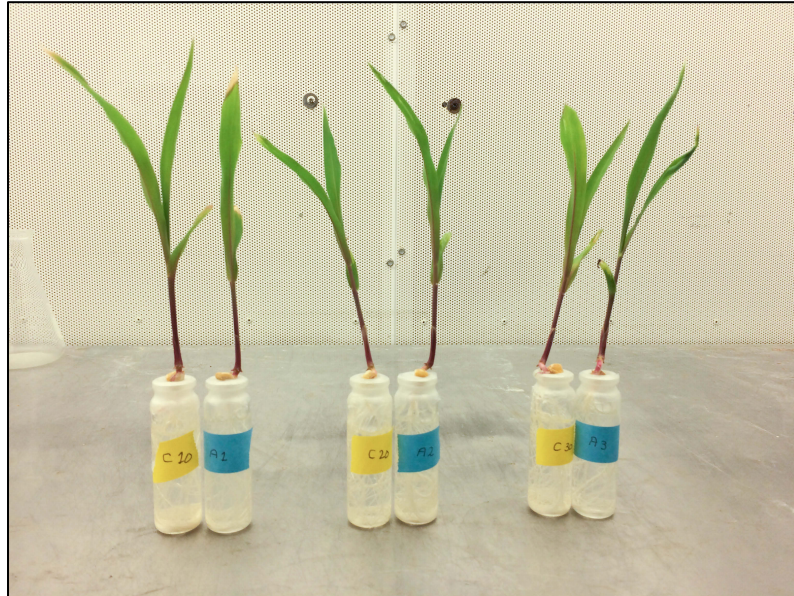


Figure 21: Maize plants exposed to nanorods on day 10. Blue label) 2.25 mg/L. Yellow label) controls

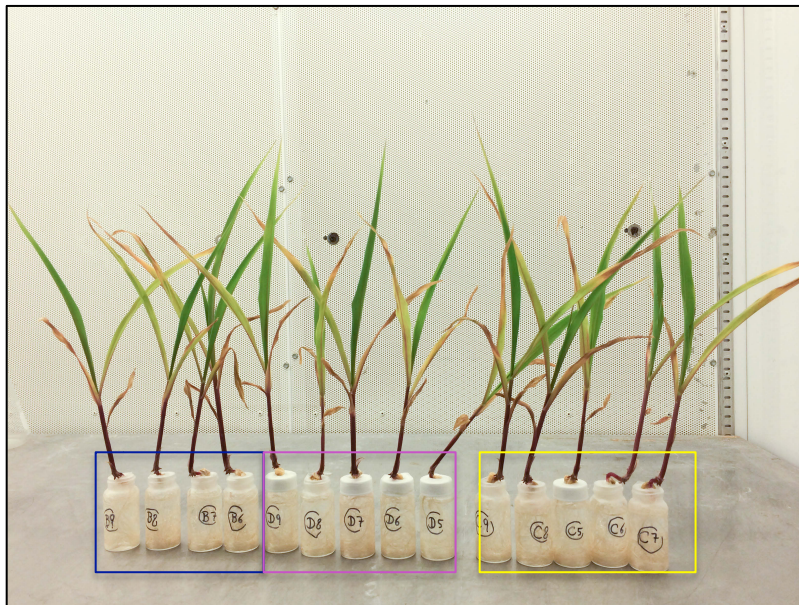


Figure 22: Maize plants exposed to nanorods on day 10. Left) 0.45 mg/L. Middle) 4.5×10^{-3} mg/L. Right) controls

6.2.2 Transpiration

The average volume of Hoagland solution added to each group of plants during the 10-day experiment was recorded as transpiration. Figure 25 indicates that control plants took-up about 27 ml of solution. By comparison, exposed plants transpired less. Plants exposed to 2.25 mg/L nanorods took-up 3 ml less than control plants. Although the differences in transpiration between exposed and controls were not statistically significant, the graph suggests some small differences. It continues to be a strong hypothesis that gold nanorods are toxic by interfering with the uptake mechanism at the root-solution interface, and that the inhibitory effect is correlated with the concentration of nanorods.

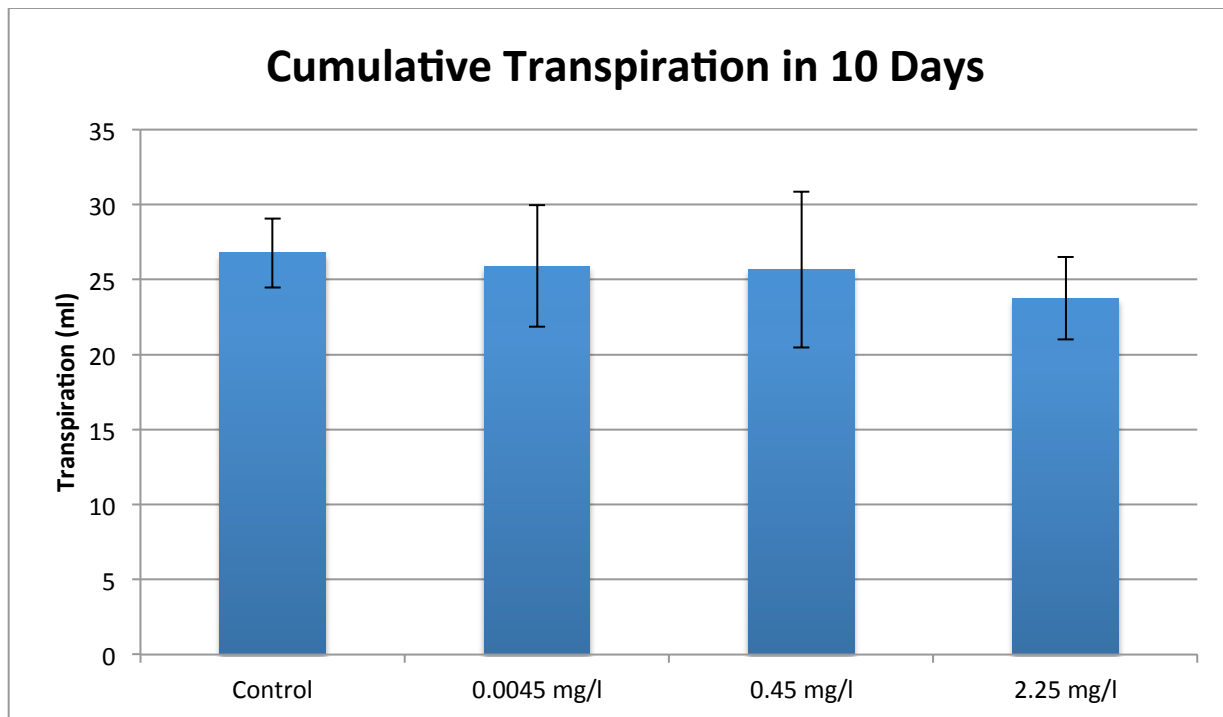


Figure 23: Cumulative transpiration of maize plants exposed to different concentrations of gold nanorod for 10 days (n=3)

6.2.3 Growth of the plants

Plant lengths were measured on day 10 before sacrificing them for analysis. The length was measured from the base of the stem to the tip of the leaf. Figure 26 indicates that exposed plant lengths were lower than that of the control plants. Clearly, lower transpiration corresponded to slower growth rate and biomass. The results of the plant lengths at the highest gold nanorod dosage (2.25 mg/L) appeared to be anomalies, measured slightly higher than that of the control plants. However, this group recorded lower transpiration, wet and dry biomasses, indicating that it was not healthier (Error bars show +/- 1 standard deviations for each group of data).

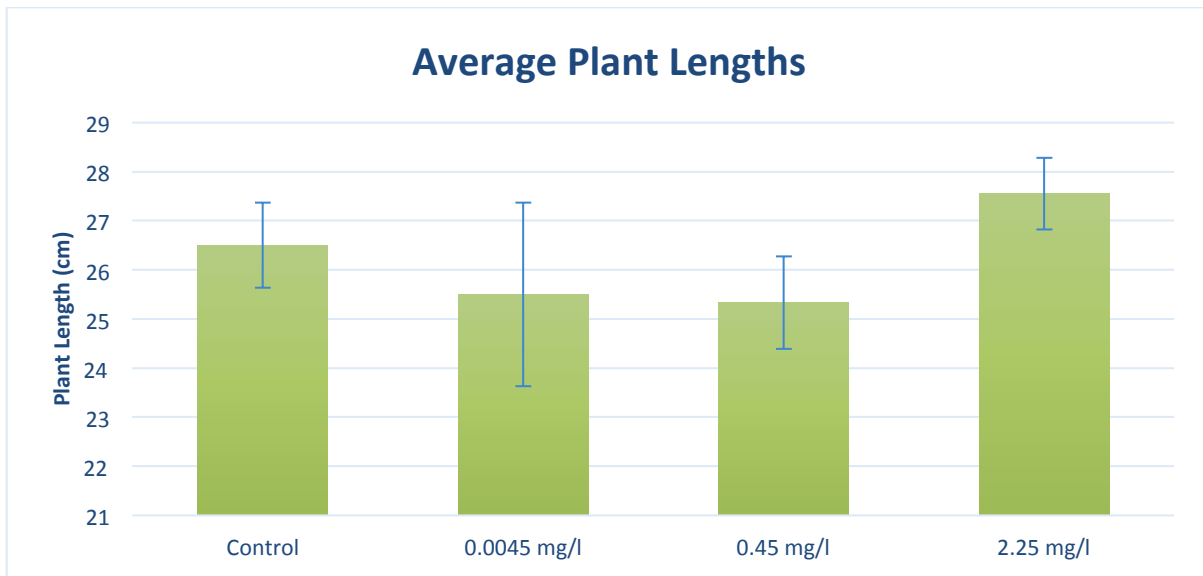


Figure 24: Average plants length on day 10 (n=3)

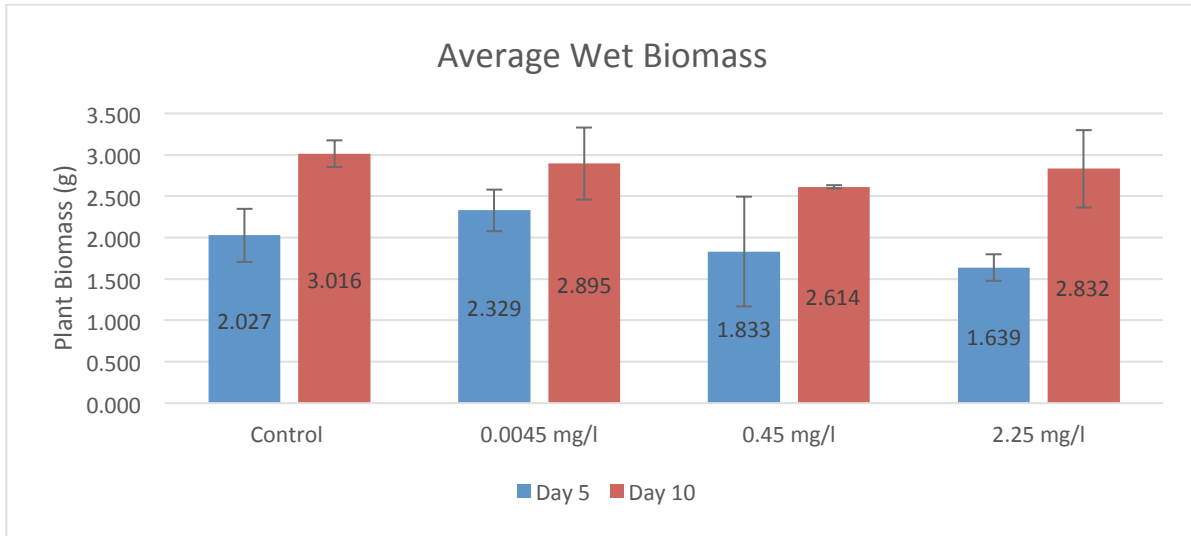


Figure 25: Average plants wet biomass on day 5 and 10. All plants were growing during this time interval. (n=3)

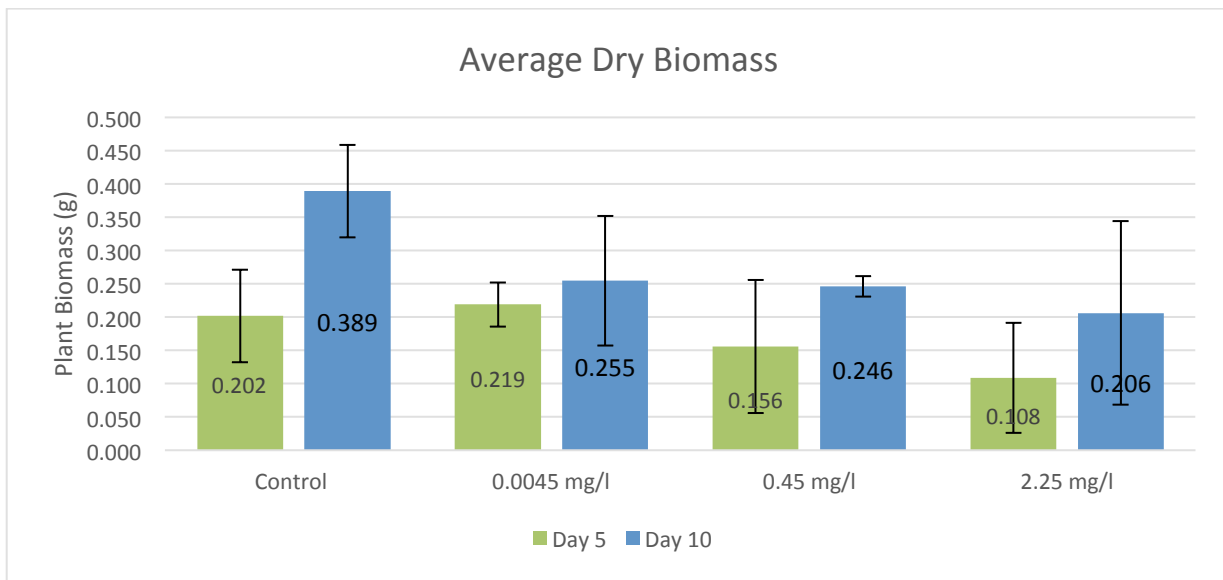


Figure 26: Average plants dry biomass on days 5 and 10. All plants were growing during this time interval. (n=3)

Average wet and dry biomasses in figures 27 and 28 demonstrate a similar trend as the transpiration measurements. According to the dry biomass and transpiration measurements, maize plants exposed to a higher concentration of gold nanorods (2.25 mg/L) had lower uptake

and growth. Still the healthy green color of the exposed plants suggests that the toxic effect of nanorods at these lower concentrations was not major. Most likely, the nanorod concentration in the solution physically restricted uptake, and thus the plant growth was lower than expected. Another observation is that there was no significant difference between plants exposed to 4.5×10^{-3} mg/L and 0.45 mg/L in all measurements, by two-tailed T-test ($p = 0.05$).

6.2.4 TEM Result

On day 10, solution and tissue samples were taken from the root, stem, and leaves of maize plants exposed to 2.25 mg/L gold nanorods, and were then prepared for TEM imaging following the procedures outlined in sections 5.3.1 and 5.3.2. Figure 29 shows the TEM image of the Hoagland solution exposed to 2.25 mg/l gold nanorods, in which gold nanorods were detectable and shown in the micrograph by red arrows.

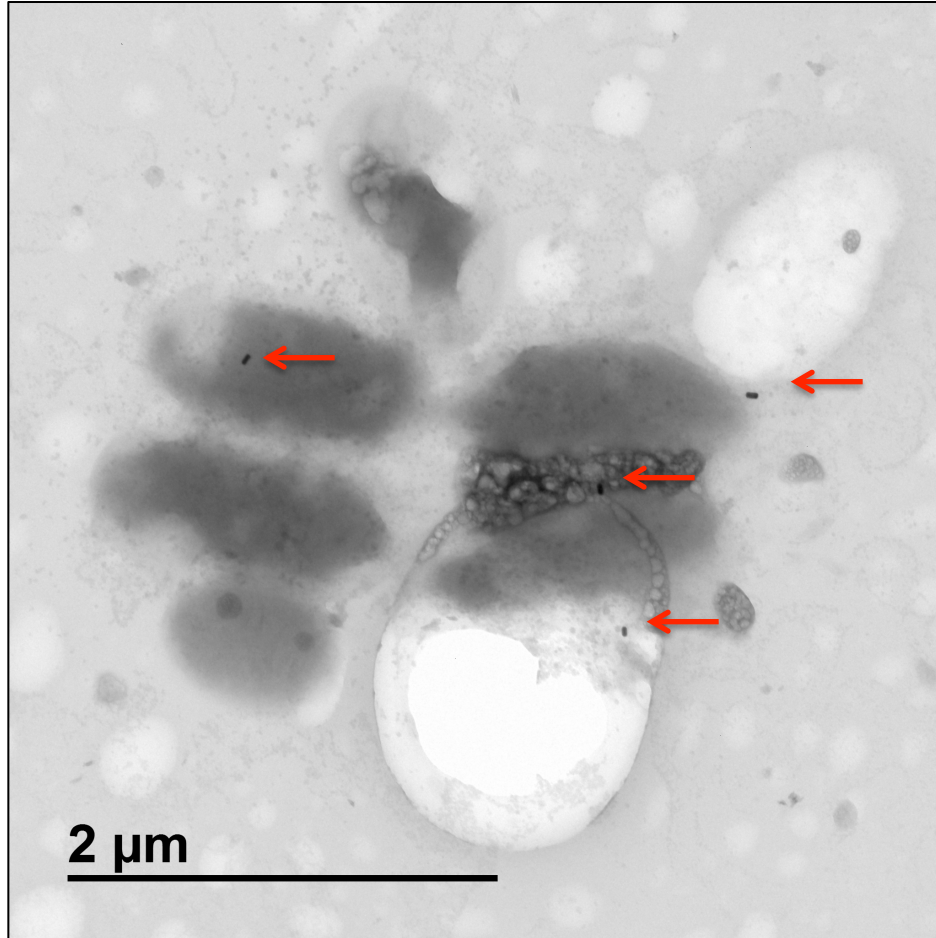


Figure 27: TEM image of solution sample exposed to 2.25 mg/L gold nanorods on day 10. Red arrows show the nanorods in the solution.

Ultra thin layers of plant tissue sample slices were observed by TEM. After a few hours investigating samples under the microscope, only one image with detectable nanorods was observed. In Figure 30, gold nanorods are shown clustered together inside of a root cell. The rod shapes and the high electron density differentiated these nanorods in the image from other dark objects. There were no dense, rod-like materials detected in control plant tissues. Nanorods detected in the root tissue were not connected or close to any organelle in the cell. The shape and

size were the same as ones shown in TEM images of stock solution. Therefore, shape or size of the nanorods did not change during the experiment or during uptake.

Although only one cluster of nanorods was found by TEM imaging during a few hours of microscopy, undoubtedly more particles were present as indicated by ICP-MS later. Lower concentrations of exposure compared to experiment 1 were the reason that exposures were less toxic, and fewer nanorods were detected in the root tissue. Further examination of the cells by TEM would likely lead to additional detection of nanorods. According to the TEM images, some translocation of gold nanorods occurred, but the number was relatively few. Detected nanorods were located inside of the root cells, which demonstrated that maize plants are able to translocate nanorods from the solution. Moreover this experiment supports the hypothesis that nanorods exhibit a toxic effect by inhibiting water and nutrient uptake, which in turn interferes with growth and photosynthesis.

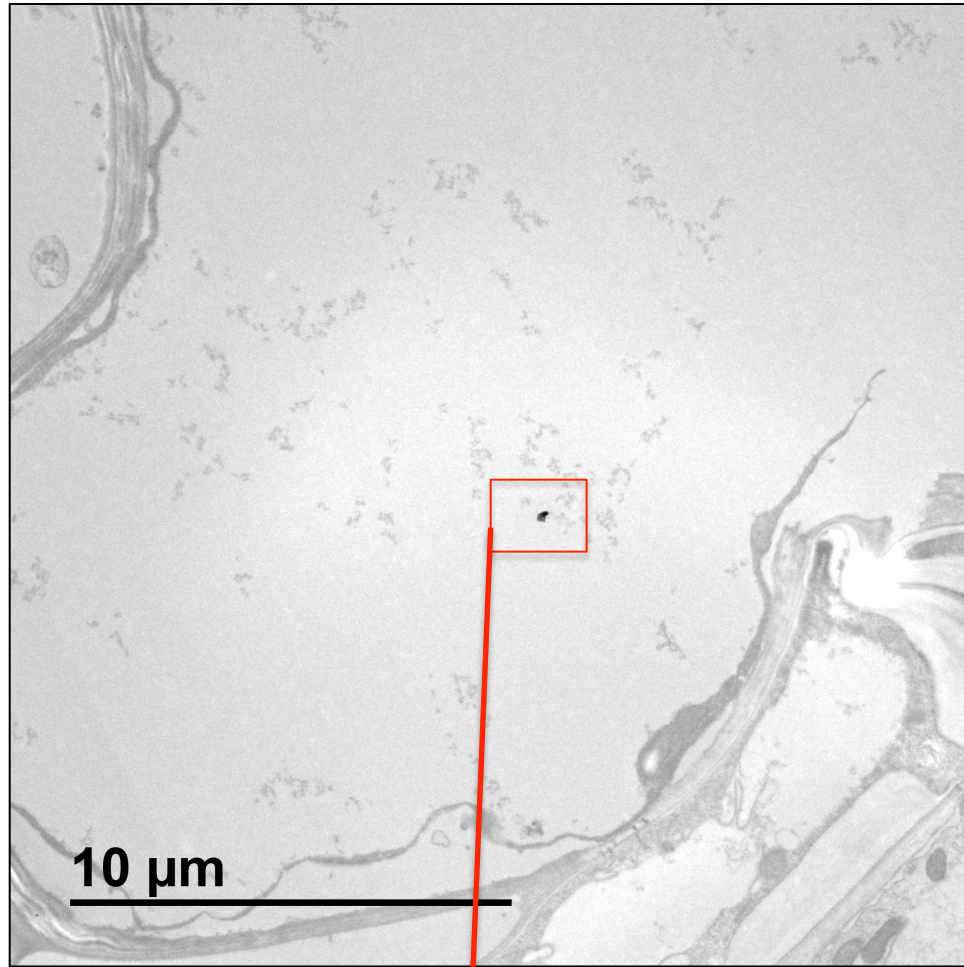
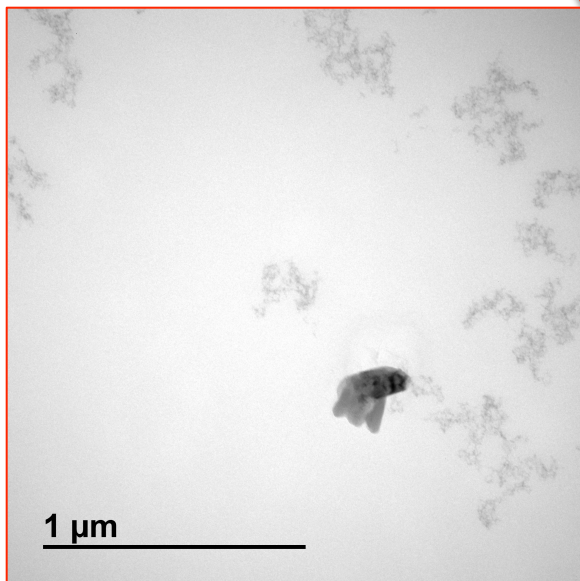


Figure 28: TEM images of detected gold nanorods in a root sample of a plant exposed to 2.25 mg/L gold nanorods (25 x 69 nm)



6.2.5 ICP-MS Result

Inductively coupled plasma mass spectrometry (ICP-MS) was used to determine the mass of gold in the sample solutions and tissues. In this analytical technique, high-temperature inductively coupled plasma converts the elements in the sample to ions, which are then separated and detected by the mass spectrometer.

While TEM is simply a visual image of small fields of the sample, ICP-MS analysis measures the total gold elements in the samples. For this analysis, samples were taken on day 10 from all three exposed groups and control plants, and were then prepared following the procedures outlined in sections 5.3.3. and 5.3.4.

After preparations, samples were analyzed by Thermo scientific X-Series ICP-MS. Triplicates of each exposure were tested. Data from the instrument was calibrated with 0, 0.5, 5 and 50 ppb standards. Knowing the mass of the samples and the volume of the solutions, Au counts per second output for each sample were then converted to grams of gold detected per gram of plant sample. Figures 31- 33 shows the results from ICP-MS analyses.

6.2.5.1 Filtered Solution Samples

Solution samples on day 10 from exposed and control plants were filtered prior to ICP-MS analysis. The filtration removed un-ionized gold species, leaving only gold ions in solution. ICP-MS analysis of the filtrate from the nanorod-exposed solutions was equivalent to that of the control plants, which indicates that there was no ionization (dissolution) of gold particles during the experiments, and that all the gold exposed in the solution remained in the form of solid nanorods.

6.2.5.2 Unfiltered Solution Samples

ICP-MS results of the unfiltered solution samples are shown in Figure 31. Gold element was undetectable in control solutions. On the other hand, solutions exposed to gold nanorods measured significant gold levels. Since the detection count is directly proportional to concentration, it is possible to measure gold concentrations through a linear equation established by calibration standards.

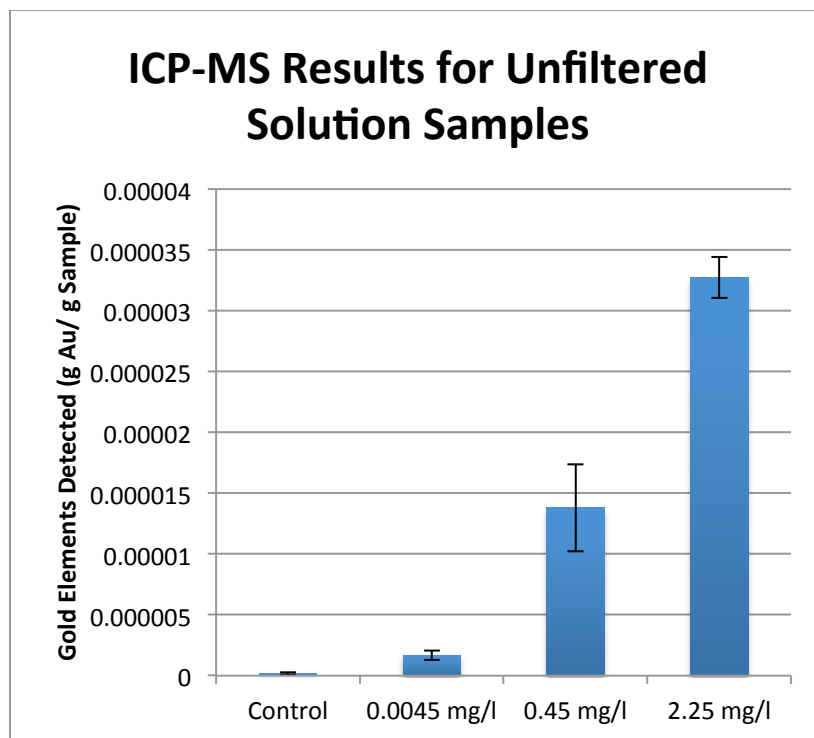


Figure 29: Gold concentrations detected in the exposure solution samples by ICP-MS. (n=3)

6.2.5.3 Root Samples

Root samples were ground by mortar and pestle, and were also examined by ICP-MS. Maize plants roots were exposed to 2.25 mg/L gold nanorods in solution and showed the highest concentration of gold detected, (figure 32) followed by plants exposed to 0.45 mg/L solution,

whereas gold concentrations of the 4.5×10^{-3} mg/L solution and control plants showed some low level of gold in root tissues, roughly equivalent to the lowest exposure concentration. This could be due to slight contamination of the chemicals which are used to prepare the Hoagland nutrient media.. It is important to note that root sample measurements may include cellular gold content as well as extra-cellular gold adsorbed to the outside of the roots or located in xylem. It was visually observed that the exposed roots were purple. Therefore, gold nanoparticles may have been trapped or adhered to the outside of root tissues.

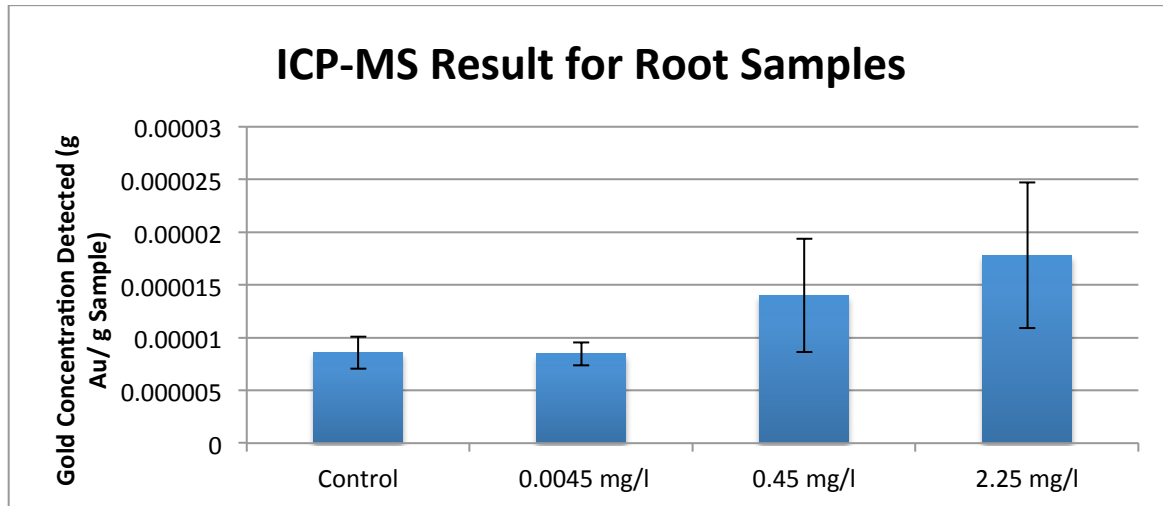


Figure 30: Gold concentration detected in root samples by ICP-MS. (n=3)

6.2.5.4 Leaf Samples

TEM imaging of leaf samples exposed to 2.25 mg/L solution showed little gold presence. ICP-MS analysis was not expected to detect significant mass quantities either. The result was consistent with that expectation and showed lower concentrations than that of control plants (not statistically significant at the 0.05 level). Because the error bars show large variance, it is reasonable to attribute the difference to sample variation. In figure 33, leaf samples from maize

plants exposed to 0.45 mg/L and 4.5×10^{-3} mg/L solutions contained higher amounts of gold compared to control plants. Though it may seem surprising that lower concentration samples took-up higher amount of gold nanorods to leaf systems, it was consistent with the Experiment 1 hypothesis that high concentrations of gold nanorods hinder uptake pathways. The samples exposed to 4.5×10^{-3} mg/L solution showed the highest concentration but also the largest variance. Only plants exposed to 0.45 mg/L solution showed statistically significant uptake of additional gold into the leaf system by two tailed T-test ($p = 0.05$).

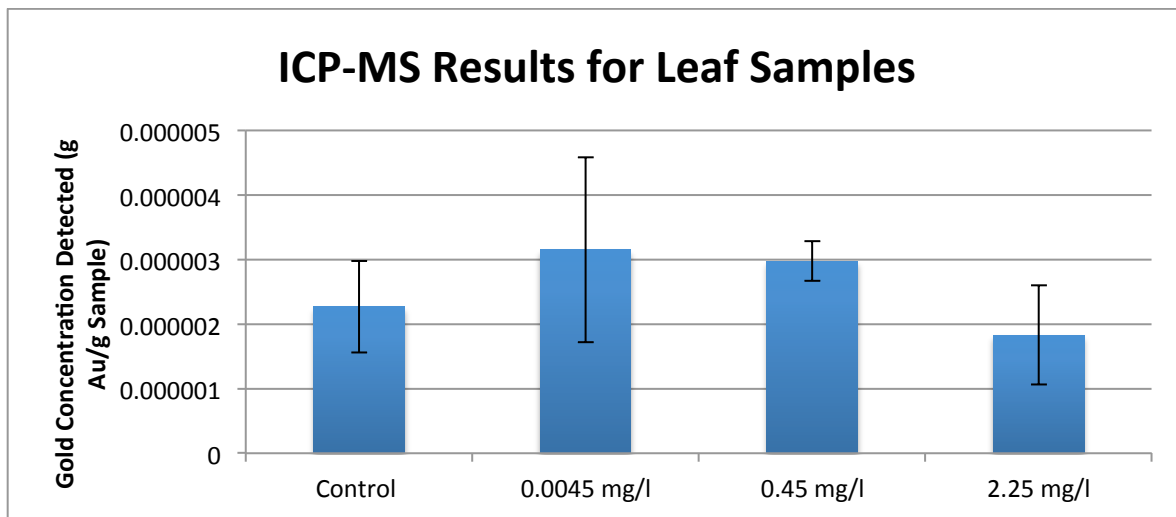


Figure 31: Gold concentration detected in leaf samples by ICP-MS. (n=3)

The main objective of experiment 2 was to investigate the possible uptake of various concentrations of gold nanorods by maize plants and the resulting translocation in the live plants (a dose-response relationship). Maize seedlings were exposed to 2.25 mg/L, 0.45 mg/L and 4.5×10^{-3} mg/L same size gold nanorods (25 x 69 nm). Transpiration and biomass measurements demonstrated that high concentrations of gold nanorods caused lower water uptake and growth. Physical and chemical properties of nanoparticles may have caused specific effects on plant systems such as the physical clogging of uptake pathways and production of reactive oxygen

species. (Navarro, et al., 2008) According to the ICP-MS results, the root system of the exposed plants was surrounded by adsorbed nanorods, which may have been toxic to maize plants and physically interfered with uptake pathways, and thus inhibited the plants' growth and nutritional uptake. Results from leaf samples of plants exposed to 0.45 mg/L showed more detectable gold, which warrants further investigation by TEM imaging for translocation to leaves.

In conclusion, as demonstrated in experiments 1 and 2, maize plants were able to uptake gold nanorods from the hydroponic system to root and leaf cells and they were bioavailable and detectable in the plant tissues by TEM and ICP-MS analysis, though very few nanorods were detected in the leaf tissue. Gold nanorods were toxic to maize plants at high concentrations after 10 days exposure. There was little change in gold nanorod characteristics, such as size, shape, or ionization, during uptake. Therefore, abrasion and dissolution did not appear to have occurred during uptake and translocation. Gold nanorods toxic effects likely caused physical growth inhibition of maize plants by hindering root uptake pathways.

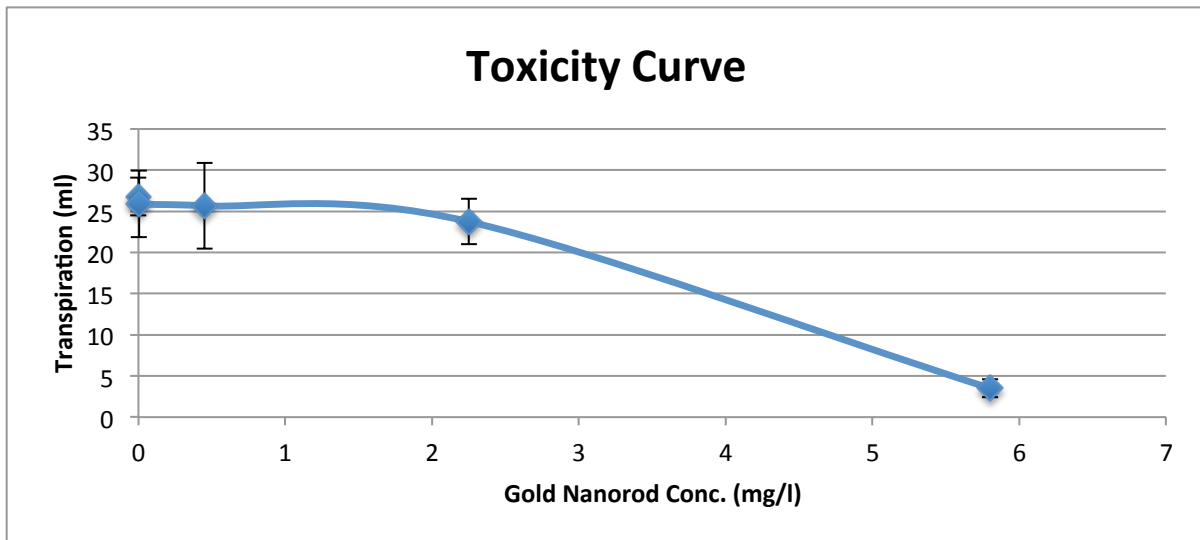


Figure 32: Toxicity curve for different concentration gold nanorods on maize plants (n=3)

Using transpiration data from experiment 1 and 2, the dose- response curve for different concentrations of 20 x 70 nm gold nanorod on maize plants was constructed. As clearly shown in figure 34, the highest concentration of 5.8 mg/L of gold nanorods was fatal to the maize plants, and transpiration ceased.

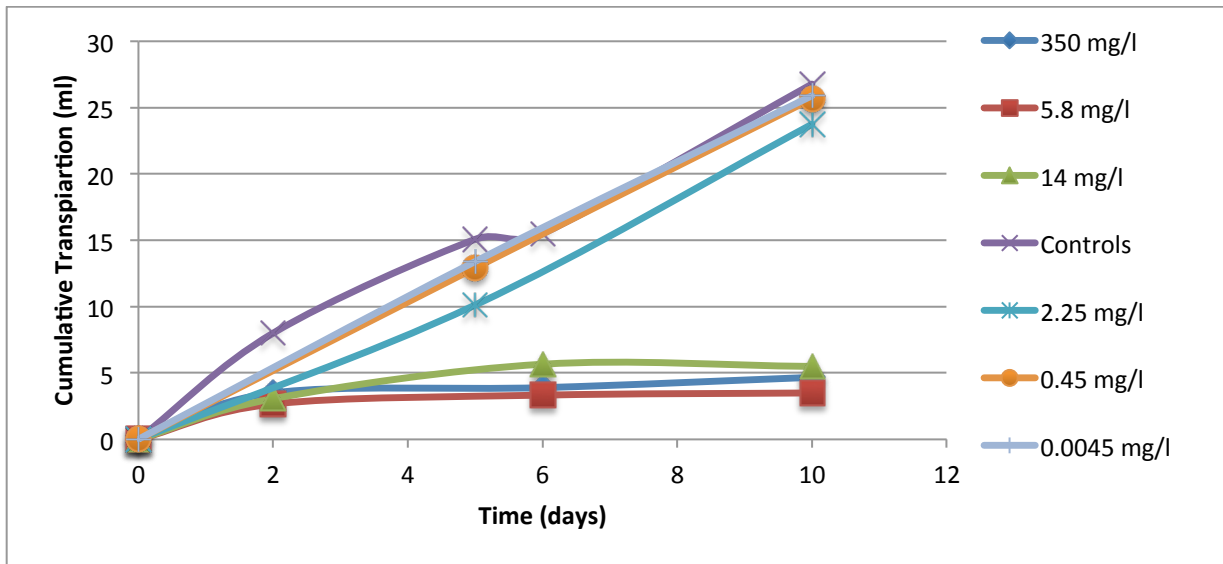


Figure 33: Plants transpiration versus time during the experiment

Figure 35 was constructed to show the cumulative transpiration measurements of both experiments and the control group. The curves clearly show that nanorods in high concentrations were toxic to the maize plants and significantly limited transpiration. Concentrations of gold nanorods at 2.25 mg/L or lower did not demonstrate clear toxic effect. The curves of low concentrations fall below the control curve, but not considerably.

CHAPTER VII

FUTURE WORKS

According to the life cycle assessments, the ENMs mostly end up in the landfill and soil. (Keller, McFerran, Lazareva, & Suh, 2013) Therefore, it is important to focus studies on soil systems, which is a more realistic approximation of natural environments. Although experiments on hydroponic systems are essential to investigate the mechanism of uptake, toxicity, and final destination of nano-materials, the disadvantage of hydroponic study is that it focuses on early growth stages. Additional studies of mature plants in soil systems are needed. Furthermore, soil systems can potentially be used to study the effects of nano-material contamination in second-generation organisms, as well as food chain. Such studies could follow the long-term pathways of nano-material contamination through the ecosystem. Since humans are the ultimate consumers, following nano-materials through the food chain can illuminate a more critical understanding of the effects on human health.

REFERENCES

- Alaaldin M. Alkilany, C. J. (2010). Toxicity and cellular uptake of gold nanoparticles: what we have learned so far? *Nanoparticle Research* , 12 (7), 2317-2333.
- Arturo A. Keller, S. M. (2013). Global life cycle releases of engineered nanomaterials. *Journal of Nanoparticle Research* , 15 (6).
- Asli, S., & Neumann, P. (2009). Colloidal suspensions of clay or titanium dioxide nanoparticles can inhibit leaf growth and transpiration via physical effects on root water transport. *Plant Cell Environ.* , 32 (5), 577- 584.
- Atha, D. H., Wang, H., Petersen, E. J., Cleveland, D., Holbrook, R. D., Jaruga, P., et al. (2012). Copper oxide nanoparticle mediated DNA damage in terrestrial plant models. *Environmental Science and Technology* , 1819- 1827.
- Card, M. (2011). Uptake and degradation of natural and synthetic estrogens by maize seedlings. *Food, Agricultural, and Environmental Sciences* .
- Cyren M. Rico, S. M.-G.-V.-T. (2011). Interaction of Nanoparticles with Edible Plants and Their Possible Implications in the Food Chain. *Agricultural and Food Chemistry* , 59 (8), 3485-3498.
- D. E. Salt, R. D. (1998). PHYTOREMEDIATION. *PLANT BIOLOGY* , 49, 643-668.
- Daohui, L., & Xing, B. (2007). Phytotoxicity of nanoparticles: Inhibition of seed germination and root growth ☆. *Environmental Pollution* , 150 (2), 243- 250.
- Eduardo Corredor, P. S.-J.-M.-P.-d.-L. (2009). Nanoparticles penetration and transport in living pumpkin plants: in situ subcellular identification. *BMC Plant Biology* , 9.
- Hao Zhu, a. J. (2008). Uptake, translocation, and accumulation of manufactured iron oxide nanoparticles by pumpkin plants. *Journal of Environmental Monitoring* , 10 (6), 713- 717.
- Harris, A. T., & Bali, R. (2008). On the formation and extent of uptake of silver nanoparticles by live plants. *Journal of nanoparticle research* , 10 (4), 691- 695.

Hoagland, D. R., & Arnon, D. I. (1950). The water-culture method for growing plants without soil. *California Agriculture Experimental Station* , 347, 23- 32.

Jonathan D. Judy, J. M. (2011). Evidence for Biomagnification of Gold Nanoparticles within a Terrestrial Food Chain. *Environmental Science and Technology* , 45 (2), 776-781.

Kráľová, E. M. (2012). Plant-Heavy Metal Interaction: Phytoremediation, Biofortification and Nanoparticles.

Lasat, M. M. (2002). Phytoextraction of Toxic Metals. *Environmental Quality* , 31 (1), 109-120.

Lee, W.-M., Youn-Joo, Yoon, H., & Kweon, H.-S. (2008). Toxicity and bioavailability of copper nanoparticles to the terrestrial plants mung bean (*Phaseolus radiatus*) and wheat (*Triticum aestivum*): Plant agar test for water-insoluble nanoparticles†. *Environmental Toxicology and Chemistry* , 27 (9), 1915-1921.

Li, N. Y., Li, Z. A., Zhuang, P., Zou, B., & McBride, M. (2009). Cadmium Uptake From Soil by Maize With Intercrops. *Water, Air, and Soil Pollution* , 199 (1-4), 45-56.

Ma, S., & Lin, D. (2013). The biophysicochemical interaction at the interfaces between nanoparticles and aquatic organisms; adsorption and internalization. *Environmental Science: Processes and Impact* , 15 (1), 145- 160.

Mamta Kumari, A. M. (n.d.). Genotoxicity of silver nanoparticles in *Allium Cepa*.

manju Rawat, D. S. (2006). Nanocarriers: Promising Vehicle for Bioactive Drugs. *Biological and Pharmaceutical Bulletin* , 29, 1790- 1798.

Martha L. López-Moreno, G. d.-V.-V.-T. (2010). X-ray Absorption Spectroscopy (XAS) Corroboration of the Uptake and Storage of CeO₂ Nanoparticles and Assessment of Their Differential Toxicity in Four Edible Plant Species. *Agricultural and Food Chemistry* , 58 (6), 3689-3693.

Mojiri, A. (2011). The Potential of Corn (*Zea mays*) for Phytoremediation of Soil Contaminated with . *Biology and Environmental Science* , 5 (13), 17-22.

Montes Castillo, M. O. (2010). *A new green chemistry method based on plant extracts to synthesize gold nanoparticles*. El Paso: Dissertation Abstracts International.

Murphy, C. J., & Jana, N. R. (2002). Controlling the Aspect Ratio of Inorganic. *Advanced Material* , 14 (1), 80-82.

Murphy, C. J., Gole, A. M., Stone, J. W., Sisco, P. N., Alkilany, A. M., Goldsmith, E. C., et al. (2008). Gold Nanoparticles in Biology: Beyond Toxicity to Cellular Imaging. *American Chemical Society* , 1721-1730.

Navarro, E., Baun, A., Behra, R., Hartmann, Q., N, Filser, J., et al. (2008). Environmental behavior and ecotoxicity of engineered nanoparticles to algae, plants and fungi. *Ecotoxicology* , 372- 386.

Onelli, E., Prescianotto-Baschong, C., Caccianiga, M., & Moscatelli, A. (2008). Clathrin-dependent and independent endocytic pathways in tobacco protoplasm revealed by labelling with charged nanogold. *Journal of Experimental Botany* , 59 (11), 3051- 3068.

P. Gonzalez-Melendi, R. F.-P.-d.-L. (2008). Nanoparticles as smart treatment - delivery system in plants: Assesment of different techniques of microscopy for their visualization in plant tissues. *Annals of Botany* , 101 (1), 187- 195.

Pei, H. (2013). Shape and Surface Property Dependent Phytotoxicity of Silver and Gold Nanoparticles to *Lactuca sativa* (Lettuce).

R. G. Haverkamp, A. T. (2007). Pick your carats: nanoparticles of gold–silver–copper alloy produced in vivo. *Journal of Nanoparticle Research* , 9 (4), 697-700.

R.A. Wuana, F. O. (2010). Phytoremediation Potential of Maize (*Zea mays* L.). A Review. *African Journal of General Agriculture* , 6 (4), 275-287.

Remya Nair, S. H. (2010). Nanoparticulate material delivery to plants. *Plant Science* (3), 154-163.

Russell, J. J. (1999). *Electron Microscopy* . Sudbury, MA: Jones and Bartlett Pub.

Salata, O. (2004). Applications of nanoparticles in biology and medicine. *Journal of nanobiotechnology* .

Schmidt, U. (2003). Enhancing Phytoextraction. *Environmental Quality* , 32 (6), 1939-1954.

Schoenfisch, D. L. (2012). Silica Nanoparticle Phytotoxicity to *Arabidopsis thaliana*. *Environmental Science and Technology* , 46 (18), 10247-10254.

Sijie Lin, J. R. (2009). Uptake, translocation and transition of carbon nanomaterials in rice plants. *Small* , 1128- 1132.

Stephen J. Klaine¹, *. P. (2008). Nanomaterials in the environment: Behavior, fate, bioavailability, and effects[†]. *Environmental Toxicology and Chemistry* , 31 (12), 1825- 1851.

Tara Sabo-Attwood, J. M. (2012). Uptake, distribution and toxicity of gold nanoparticles in tobacco (*Nicotiana xanthi*) seedlings. 6.

Torney, F., Trewyn, B. G., Lin, V. S., & Wang, K. (2007). Mesoporous silica nanoparticles deliver DNA and chemicals into plants. *Nature Nanotechnology* , 295- 300.

Wang, J., Koo, Y., Alexander, A., Yang, Y., Westerhof, S., Zhang, Q., et al. (2013). Phytostimulation of Poplars and *Arabidopsis* Exposed to Silver Nanoparticles and Ag⁺ at Sublethal Concentrations. *Environmental Science and Technology* , 47 (10), 5442-5449.

Wendy Ann Peer, I. R. (2006). Phytoremediation and hyperaccumulator plants. *Molecular Biology of Metal Homeostasis and Detoxification* , 4, 299-340.

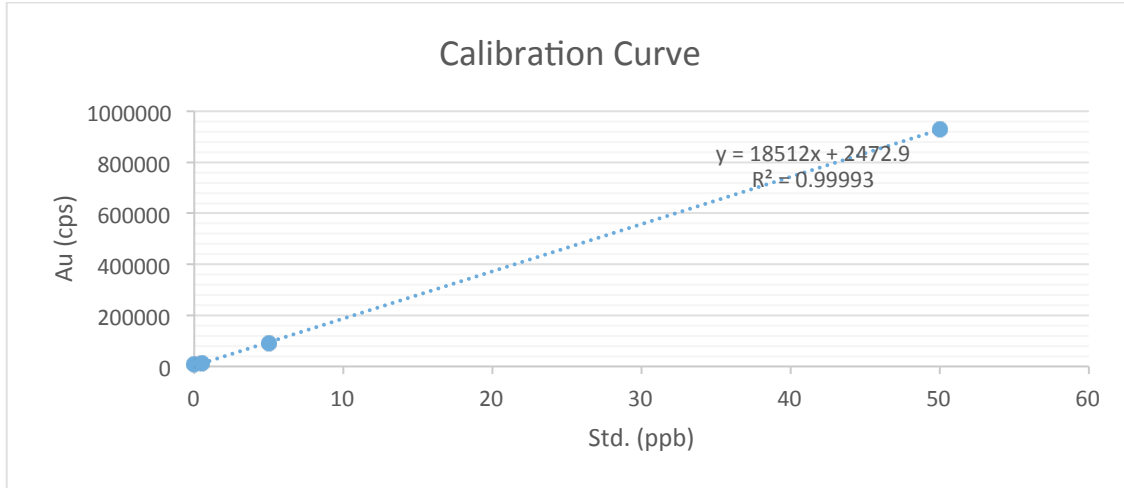
Xingmao Ma, J. G.-L. (2010). Interactions between engineered nanoparticles (ENPs) and plants: phytotoxicity, uptake and accumulation. *Science of The Total Environment* , 408 (16), 3053-3061.

Zhai, G., Walters, K., Peate, D., Alvarez, P. J., & Schnoor, J. L. (2014). Transport of Gold Nanoparticles through Plasmodesmata and Precipitation of Gold Ions in Woody Poplar. *Environmental Science and Technology* , 146- 151.

Zhi Ping Xu, Q. H. (2006). Inorganic nanoparticles as carriers for efficient cellular delivery. *61* (3), 1027- 1040.

APPENDIX

A. Calibration curve from standards, used to calibrate ICP-MS data.



B. Raw and calculated data from ICP-MS analysis for experiment 2.

No.	Sample	Average Au (cps)	Calibrated (ng/ml)	g Au/g sample
1	C7 S	346.3795625	0.019629009	4.05653E-08
2	C8 S	1335.005438	0.073029067	1.50922E-07
3	C9 S	2809.362563	0.152665619	3.15499E-07
4	D7 S	12304.25069	0.66552654	1.37538E-06
5	D8 S	20003.57081	1.081400889	2.23482E-06
6	D9 S	12892.37631	0.697293808	1.44103E-06
7	B7 S	99029.77469	5.349955842	1.10562E-05
8	B8 S	168864.0619	9.122014702	1.88516E-05
9	B9 S	102714.1713	5.548966404	1.14675E-05
10	A7 S	272579.2	14.72412824	3.04289E-05
11	A8 S	298069.3894	16.10096616	3.32743E-05
12	A9 S	308576.9113	16.66852391	3.44472E-05
34	A6 R	1265739.363	68.36910324	1.08137E-05
31	A6 L	343557.9219	18.55800308	1.12672E-06
35	A7 R	2122533.613	114.6483519	2.7229E-05
32	A7 L	630537.4513	34.05903731	2.90214E-06
36	A8 R	2432536.263	131.3929668	1.54206E-05
33	A8 L	568589.17	30.71293653	1.46388E-06
30	B9 R	1282154.556	69.25576049	1.86967E-05
27	B9 L	887486.6331	47.9379996	3.40692E-06
28	B7 R	946219.4381	51.11041828	6.47934E-06
25	B7 L	879165.1563	47.48851981	2.72204E-06
29	B8 R	1037802.856	56.05724394	1.68284E-05
26	B8 L	730852.2506	39.47748351	2.79774E-06
22	D6 R	980976.4825	52.98780005	7.09948E-06
19	D6 L	814472.4931	43.99418282	2.89211E-06
23	D7 R	769938.4806	41.58870375	9.73488E-06
20	D7 L	443053.2975	23.93218857	1.53581E-06
24	D8 R	834652.1019	45.08417278	8.53714E-06
21	D8 L	789095.0194	42.62343317	5.01678E-06
16	C5 R	791614.6688	42.75953058	9.78445E-06
13	C5 L	702926.1413	37.96907077	2.33539E-06
17	C7 R	918527.47	49.61465255	9.48632E-06
14	C7 L	872718.3363	47.14029854	3.13758E-06
18	C8 R	885590.1481	47.83556205	6.42227E-06
15	C8 L	500409.6794	27.03026056	1.40064E-06
37	NR S	14090879.13	761.1116516	0.001572913

C. Transpiration data for experiment 1.

	Day2	Day6	Day 10	Total
S1	3.5			3.5
S2	4			4
S3	3			3
S1	0	3		3
S2	2	1.5		3.5
S3	3	2.2		5.2
S1	3.5	1	0.5	5
S2	2.5	1.2	0	3.7
S3	4	2	1	7
S4	0	3	0	3
Total	25.5	13.9	1.5	40.9
Average	2.55	1.985714286	0.375	4.675
STNDEV				1.522128444
M1	2.5			2.5
M2	3			3
M3	2.5			2.5
M1	2.5	1.5		4
M2	2.5	1		3.5
M3	1.5	1		2.5
M1	3	1.5	0.5	5
M2	1.5	1	0	2.5
M3	2	0	1	3
Total	21	6	1.5	28.5
Average	2.33	1.00	0.50	3.50
STNDEV				1.08
L1	3.2			3.2
L2	2.5			2.5
L3	3.5			3.5
L1	2	2		4
L2	3	3		6
L3	4	3		7
L1	2	2	0	4
L2	3.5	2	1	5.5
L3	4	3	1.5	7
Total	27.7	15	2.5	42.7

Average	3.08	2.50	0.83	5.50
STNDEV				1.22
C1	9			9
C2	8			8
C3	8			8
C1	7			7
C2	9	7		16
C3	8	7		15
C1	7	7	6	14
C2	9	6	6	15
C3	8	8	7	16
Total	73	35	19	108
Average	8.11	7.00	6.33	15.00
STNDEV				0.82

D. Transpiration data for experiment 2.

		Day 2	Day 5	Day 8	Day 10	Sum (mL)
Sample No.	Sample taken on day	Evapotranspiration (mL)				
A1	5	4.8	4.5			9.3
A2	5	4.4	5			9.4
A3	5	4	7			11
A4	5	3.8	4.5			8.3
A5	5	5.1	7.5			12.6
A6	10	4	8.5	7	4	23.5
A7	10	5.2	6	6.5	4	21.7
A8	10	4.8	6	10	7.5	28.3
A9	10	4.5	6	6.5	4.5	21.5
Total			50.6		95.00	145.60
Average			10.12		23.75	16.18
B1	5	6.8	7			13.8
B2	5	4.9	5			9.9
B3	5	10	5			15
B4	5	6.1	6.3			12.4
B5	5	7.5	6			13.5
B6	10	8.1	10	9.5	7	34.6
B7	10	6	6.5	6	4.3	22.8
B8	10	6.2	6.5	6.5	4.5	23.7
B9	10	5.2	6	6.5	3.9	21.6
Total			64.6		102.70	167.30
Average			12.92		25.68	18.59
C1	5	6.8	8			14.8
C2	5	6.6	6			12.6
C3	5	7.7	8.5			16.2
C4	5	7.2	9.5			16.7
C5	10	6.8	6.5	6.5	5	24.8
C6	10	6.8	8	7.5	6	28.3
C7	10	7.6	8.5	8.5	5	29.6
C8	10	6.8	7	8	6	27.8
C9	10	6.4	6.5	6	4.5	23.4
Total			60.3		133.9	194.2
Average			15.075		26.78	21.57777778
D1	5	9.1	10			19.1

D2	5	6.2	6			12.2
D3	5	6.4	6			12.4
D4	5	4.9	5			9.9
D5	10	5.9	6.5	8	4	24.4
D6	10	8.4	6.5	6.5	4	25.4
D7	10	8.5	9.5	9	5.5	32.5
D8	10	5.8	5.2	5	4	20
D9	10	7.7	5	9.5	5	27.2
Total			53.6		129.5	183.1
Average			13.4		25.9	20.34444444

E. General method of preparing plant samples for TEM

½ strength Karnovsky's fixative	1 hour
0.1 M Cacodylate buffer	3 changes in 30 min
1% OsO ₄ in 0.1 M Cacodylate buffer	1-2 hours
0.1 M Cacodylate buffer	3 x 20 min
dd H ₂ O rinse	1 min
2.5% Uranyl Acetate	1 hour
15% Acetate	1 hour
30% Acetate	1 hour
50% Acetate	1 hour
75% Acetate	1 hour
95% Acetate	1 hour
100% Acetate	2 x 1 hour
1 part Acetate, 1 part Propylene Oxide	30 min
Propylene Oxide	1 hour
25 part PO and 1 part Spurr's	1 hour
10 parts PO and 1 part Spurr's	1 hour
1 part PO and 1 part Spurr's	1 hour
1 part PO and 2 parts Spurr's	1 hour
1 part PO and 3 parts Spurr's	1 hour
100% Spurr's	1 hour
100% Spurr's	5 hour
Embed in fresh Spurr's in flat embedment mold	
Place in a 70°C oven	24 hours
Microtomy	
Uranyl and Lead staining	
Examination in the microscope	